Mucosal SARS-CoV-2 vaccination of rodents elicits superior systemic T central memory function and cross-neutralising antibodies against variants of concern

Aled O'Neill,[a] Chinmay Kumar Mantri,[a] Chee Wah Tan,[a,b] Wilfried A. A. Saron,[a] Santhosh Kambaiah Nagaraj,[c] Monica Palanichamy Kala,[a] Christy Margarat Joy,[c] Abhay P. S. Rathore,[a,d] Shashank Tripathi,[c] Lin-Fa Wang,[a,e] and Ashley L. St. John[a,d,e,f,*]

[a]Program in Emerging Infectious Diseases, Duke-National University of Singapore Medical School, 169857, Singapore
[b]Infectious Diseases Translational Research Programme, Department of Microbiology and Immunology, Yong Loo Lin School of Medicine, National University of Singapore, 117545, Singapore
[c]Centre for Infectious Disease Research, Microbiology and Cell Biology Department, Indian Institute of Science, Bengaluru, 560012, India
[d]Department of Pathology, Duke University Medical Centre, Durham, North Carolina, 27705, USA
[e]SingHealth Duke-NUS Global Health Institute, Singapore
[f]Department of Microbiology and Immunology, Yong Loo Lin School of Medicine, National University of Singapore, Singapore

eBioMedicine
2024;99: 104924
Published Online xxx
https://doi.org/10.1016/j.ebiom.2023.104924

Summary

Background COVID-19 vaccines used in humans are highly effective in limiting disease and death caused by the SARS-CoV-2 virus, yet improved vaccines that provide greater protection at mucosal surfaces, which could reduce break-through infections and subsequent transmission, are still needed.

Methods Here we tested an intranasal (I.N.) vaccination with the receptor binding domain of Spike antigen of SARS-CoV-2 (S-RBD) in combination with the mucosal adjuvant mastoparan-7 compared with the sub-cutaneous (S.C.) route, adjuvanted by either M7 or the gold-standard adjuvant, alum, in mice, for immunological read-outs. The same formulation delivered I.N. or S.C. was tested in hamsters to assess efficacy.

Findings I.N. vaccination improved systemic T cell responses compared to an equivalent dose of antigen delivered S.C. and T cell phenotypes induced by I.N. vaccine administration included enhanced polyfunctionality (combined IFN-γ and TNF expression) and greater numbers of T central memory (T_{CM}) cells. These phenotypes were T cell-intrinsic and could be recalled in the lungs and/or brachial LNs upon antigen challenge after adoptive T cell transfer to naïve recipients. Furthermore, mucosal vaccination induced antibody responses that were similarly effective in neutralising the binding of the parental strain of S-RBD to its ACE2 receptor, but showed greater cross-neutralising capacity against multiple variants of concern (VOC), compared to S.C. vaccination. I.N. vaccination provided significant protection from lung pathology compared to unvaccinated animals upon challenge with homologous and heterologous SARS-CoV-2 strains in a hamster model.

Interpretation These results highlight the role of nasal vaccine administration in imprinting an immune profile associated with long-term T cell retention and diversified neutralising antibody responses, which could be applied to improve vaccines for COVID-19 and other infectious diseases.

Funding This study was funded by Duke-NUS Medical School, the Singapore Ministry of Education, the National Medical Research Council of Singapore and a DBT-BIRAC Grant.

Keywords: Mucosal vaccine; T cell; SARS-CoV-2; COVID-19

Abbreviations: Intra-nasal, I.N.; sub-cutaneous, S.C.; mastoparan-7, M7; T memory, T_{MEM}; T central memory, T_{CM}; T effector memory, T_{EM}; receptor binding domain of Spike antigen of SARS-CoV-2, S-RBD; variants of concern, VOC; angiotensin-converting enzyme 2, ACE2; lymph nodes, LNs; popliteal lymph node, PLN

*Corresponding author. Program in Emerging Infectious Diseases, Duke-National University of Singapore Medical School, 8 College Rd., Level 9, 169857, Singapore.
E-mail address: ashley.st.john@duke-nus.edu.sg (A.L. St. John).

Research in context

Evidence before this study

When an immune response is triggered, it can be imprinted with information relating to the location that experienced the challenge, whether during infection or following vaccination. These polarised immune responses are often retained during the conversion of lymphocytes from activated to memory immune phenotypes. With respect to pathogens that infect mucosal surfaces, this can be illustrated by the importance of IgA in typifying antibody responses at mucosal surfaces, which has the potential to guard against subsequent infections. SARS-CoV-2 is an important human pathogen that initiates infection in the nasal mucosae and can penetrate into the lung during infection. Studies have shown that there are unique advantages of vaccinating against SARS-CoV-2 at mucosal surfaces to imprint the type of mucosal protection required to limit SARS-CoV-2-induced disease. However, aside from the known role of IgA, there have been few investigations into the contributions of other aspects of immunity on protection from disease following mucosal vaccination.

Added value of this study

Here, using an adjuvant that works well for peripheral and mucosal challenges, we observed that T cell phenotypes are differentially-induced by mucosal versus sub-cutaneous vaccination with the same vaccine formulation. Specifically, in addition to the improved IgA responses which are expected, mucosal vaccination also improves detection of antigen-specific T cells compared to sub-cutaneous vaccination, and this is typified by an abundance of T central memory cells, which are known to be associated with improved recirculation of T cells through secondary lymphoid tissues. Furthermore, IgG antibodies are induced by mucosal vaccination that have greater capacity to cross-neutralize evolutionarily divergent SARS-CoV-2 variants of concern. Hamster SARS-CoV-2 model studies also indicate a protection from severe disease following mucosal vaccination that supports these immunological changes have meaningful functional outcomes.

Implications of all the available evidence

Together these data support that T central memory cell induction resulting from mucosal vaccination, coupled with improved antibody cross-neutralising responses, are ways that mucosal vaccination may improve vaccine-induced immunity to SARS-CoV-2, beyond IgA responses. This may have implications for improving vaccines to prevent COVID-19 or other pathogens that target the mucosae.

Introduction

SARS-CoV-2 emerged in 2019 as a novel Coronavirus infecting humans and in 2020 it began a major ongoing global pandemic. The disease it induces in humans, COVID-19, is characterised by fever, cough, fatigue and dyspnea, with severe cases leading to pneumonia and death.[1,2] Vascular complications and coagulation disorders also occur.[3] The elderly and those with pre-existing conditions, such as diabetes and hypertension, are most at risk for developing life-threatening complications.[1,4] The widespread worldwide distribution of active COVID-19 infection clusters and the severity of disease outcomes in patients in multiple age groups has necessitated unprecedented advances in vaccine technologies and distribution. Although a multitude of vaccines are now available that show protection in terms of significantly reducing the incidence of infections, hospitalisations, deaths and reducing transmission,[5–9] breakthrough infections often occur,[10] suggesting that there are limitations to the duration of protective immune responses induced by the current vaccine regimens. Furthermore, new variants of concern (VOC) continue to circulate, even in populations with high levels of vaccine coverage.[11] This is thought to be at least partially attributable to immune pressure on the SARS-CoV-2 virus leading to diversification of antigenic properties through virus mutation.[11]

Among the first vaccines approved against SARS-CoV-2 were mRNA-based vaccines, which initial analyses showed can be >90% effective a few weeks following the vaccine protocol completion.[7,12] Most strategies have used the Spike (S) protein as antigen, which is found on the virus surface. Often, the region of the S-protein containing its receptor binding domain (RBD) that allows its entry into host cells via binding to the angiotensin-converting enzyme 2 (ACE2) receptor is used. Importantly, ACE2 is expressed by the type I and II alveolar cells of the lung that are key targets of lower respiratory tract infection by SARS-CoV-2,[13–15] so that neutralising antibodies against this protein are effective in preventing cellular entry and infection by the virus. For human vaccinees who were given mRNA vaccines, there are strong correlations between the titre of vaccine-induced antibody responses and protection from symptomatic disease.[16] Notwithstanding their efficacy, risk of breakthrough infection appeared to increase in the months following completion of the two-dose mRNA vaccine,[10] likely owing to the natural time-related decay in specific antibodies. Complicating this phenomenon of waning protection over time has been the emergence of VOC, for which vaccine-induced antibodies show decreased neutralization.[11] Despite the loss of antigen-specificity and neutralization capacity of vaccine-induced antibodies to VOC such as Omicron,[17]

vaccinees remain highly protected against severe disease and death,[18] which could possibly point to a protective role for T cells in vaccine-induced protection. Indeed, T cells are highly cross-reactive to VOC and even to SARS-CoV-1 and seasonal coronaviruses.[19–21] In primates with SARS-CoV-2 infection, CD8 T cell activation correlated with viral control in the absence of neutralising antibodies.[22] In humans, rapid induction of SARS-CoV-2-specific T cell responses were also associated with mild disease.[23,24] Boosting of mRNA vaccines has been shown to lead to a surge in vaccine protection that correlated with the boost in S-specific antibody titres.[25] These observations highlight outcomes of COVID-19 vaccines that could be further improved as our understanding of functional correlates of COVID-19 protection grows.

mRNA vaccines also have limitations for world-wide use given that they are difficult to distribute and require strict cold chain adherence and storage near –80 °C.[26] Several alternative vaccine approaches are also being developed for SARS-CoV-2, including subunit vaccines,[27] which involve use of more-stable protein antigens and have an advantage for stability at multiple temperatures. Although subunit vaccines have been used effectively in the context of many viral vaccines, including those approved for hepatitis B and influenza viruses,[28,29] usually, the protein components of subunit vaccines are not sufficient, alone, to establish immune memory.[30] For this reason, adjuvants, or substances that promote immune activation, are often added to the subunit vaccine formulation to induce long-term memory responses. Alum and AS04 (aluminium salt combined with the TLR4 agonist 2-O-desacyl-4′-monophosphoryl lipid A) are two human-approved adjuvants, but these are not used at mucosal surfaces.[31,32] Currently, there are no mucosal adjuvants approved for use in humans, but there are adjuvants that have been used in mucosal vaccine formulations in experimental settings, including the most widely studied experimental mucosal adjuvant, Cholera toxin,[33] and mast cell activating compounds, such as mastoparan.[33–35] Cholera toxin causes toxicity so it cannot be used in humans.[33] Mastoparan is a short 14aa peptide that is of insufficient length to trigger immune responses itself. Its analogue, mastoparan-7 (M7) has greater cell-activating activity and appears to work *in vivo* primarily through inducing mast cell degranulation responses through the MrgX2 receptor.[36] However, as a cationic amphiphilic peptide, it can also stimulate other cell types.[37] In the absence of antigen, it is insufficient to trigger adaptive immune responses,[34,35,38] but M7 is effective in enhancing the titre of antigen-specific antibodies in animal models when delivered in combination with vaccine antigens, both through sub-cutaneous (S.C.) injection as well as application to the nasal mucosae.[37] In a haptenated cocaine vaccination strategy, M7 augmented antibody responses that prevented the psychoactive effects of cocaine. This was likely through its enhanced titres of IgA and improved antigen-specific IgG avidity compared to similar subcutaneous vaccinations with Alum used as adjuvant.[35] However, it is unknown if M7 works differently in the skin compared to mucosal sites, induces site-specific responses, or influences T cell phenotypes and functions that are particularly important for combatting certain types of viral pathogens. Prior studies also established the adjuvant activity of M7 during homologous challenges, but whether mucosal vaccines generally or M7-adjuvanted vaccines specifically induce responses that are more broadly protective against diverse viral isolates compared to conventional approaches is also unknown. For vaccines against SARS-CoV-2, mucosal vaccines have shown promise in experimental studies, with multiple platforms, including unadjuvanted S protein and viral vector-based systems evoking protective immune responses.[39–45]

Given that SARS-CoV-2 infection is initiated at the mucosal surface of the nasal passages and lung airways, we planned this study with the aim of testing whether delivery of an adjuvanted subunit vaccine intra-nasally (I.N.) has advantages for the induction of SARS-CoV-2-specifc and protective immune responses. We found that mucosal administration of adjuvanted SARS-CoV-2 subunit vaccines is a promising strategy to improve systemic immune responses, through preferential induction of central memory T (T_{CM}) cells that are polyfunctional. These T_{CM} responses are T cell intrinsic and are maintained following transfer to new hosts to promote improved memory recall upon lung antigen challenge in both the draining brachial lymph nodes (LNs) and lungs. Furthermore, the improved polyfunctional response following I.N. vaccination is extended to antibodies, which show improved breadth of neutralising responses against multiple variants compared to vaccination S.C. with the same adjuvant. Finally, the I.N. vaccination resulted in improved protection of clinical disease and improved lung histopathology compared to unvaccinated animals in a hamster challenge model.

Methods

Viruses

SARS-CoV2 Wuhan isolate (Hong Kong/VM20001061/2020, Cat No.: NR-52282) and Omicron variant (USA/PHC658/2021, Cat No.: NR-56461) were obtained from BEI resources, NIAID, NIH. They were propagated (at 0.01 MOI) and titrated by plaque assay in Vero-E6 cells.

Animal studies

C57BL/6 mice purchased from InVivos were used for all experiments and immunisations began when they were 8–10 weeks old. Male Syrian golden hamsters (6–7-weeks old) were used for SARS-CoV-2 challenge studies and were procured from the Advanced Centre

for Treatment, Research and Education in Cancer, Tata Memorial centre, Navi Mumbai, India. The animals were housed separately based on groups and maintained in individually ventilated cages at 23 ± 1 °C temperature and 50 ± 5% relative humidity, given access to standard pellet feed and water ad libitum and maintained on a 12 h day/night light cycle at the Viral Biosafety level-3 facility, Indian Institute of Science, Bangalore. The hamster study complied with institutional biosafety guidelines (IBSC/IISc/ST/17/2020; IBSC/IISc/ST/18/2021), following the Indian Council of Medical Research and Department of Biotechnology recommendations.

Ethics

All mouse studies were conducted at the vivarium in Duke-NUS Medical School and approved by the SingHealth IACUC. All hamster experiments were reviewed and approved by the Institutional Animal Ethics Committee (Ref: IAEC/IISc/ST/784/2020) at the Indian Institute of Science. The experiments were performed according to the guidelines of CPCSEA (The Committee for Control and Supervision of Experiments on Animals).

Mouse vaccinations

Mice were vaccinated with 1 μg of recombinant S-RBD protein (Sino Biological) either with or without 20 μg of M7. For some groups, S-RBD was resuspended in alum (Invitrogen, VAC-alu-250). Footpads were injected with a 20 μL volume of vaccine or vehicle control (PBS). For nasal inoculations, the same doses of 1 μg S-RBD + 20 μg M7 (Sigma, M212) were instilled in a volume of 12 μL per mouse (6 μL per nare).

Hamster vaccinations

The hamsters were vaccinated either I.N. or S.C. with S-RBD (3 μg/animal) and M7 (60 μg/animal) on days 0 and 14. For I.N. immunisation, the vaccine formulation was given in a total volume of 20 μL (10 μL per nostril). For S.C. immunisation, hamsters were injected in the neck region with a volume of 90 μL. Weight was recorded before the administration of each vaccine dose. Post-immune sera were collected one day before infection, i.e., week 5 after the first vaccine dose. Blood collection was performed retro-orbitally and blood was allowed to clot for 30 min at room temperature. Following the incubation, samples were centrifuged at 3000 rpm for 15 min and cleared serum was collected and stored at –80 °C.

Hamster SARS-CoV-2 infections

Animals were infected under anaesthesia following intraperitoneal injection of Ketamine (150 mg/kg) (Bharat Parenterals Limited) and Xylazine (10 mg/kg) (Indian Immunologicals Ltd.). They were challenged with Hong Kong (Wuhan-like) or Omicron SARS CoV-2 viruses I.N. with 10^5 plaque-forming units (PFU) in 100 μL PBS. Bodyweight and clinical signs of animals were recorded daily. Hamsters were observed daily until day 4 post-infection for the following clinical signs and were scored based on severity: Lethargy (none = 0, mild = 1, severe = 2), piloerection (none = 0, mild = 1, moderate = 2, severe = 3), abdominal respiration (none = 0, mild = 1, severe = 2), hunched back (none = 0, mild = 1, severe = 2). Bodyweight loss was also considered as a clinical sign, with scoring done from a scale of 1–3 (1–5% = 1; 5.1–10% = 2; 10.1–15% = 3). On day 4, all animals were euthanised using an overdose of Xylazine (Indian Immunologicals Ltd.). The lung samples were harvested for virological (left lobe) and histopathological analysis (right lobe).

Quantification of lung viral load by qRT PCR

Lung samples from hamsters were processed using a tissue homogeniser and total RNA was isolated using TRIzol (15596018, Thermo Fisher) according to the manufacturer's instructions. A 10 μL reaction mixture with 100 ng of RNA per sample, in a 384 well block was used to quantify viral RNA using AgPath-ID One-Step RT-PCR kit (AM1005, Applied Biosystems). The following primers and probes targeting the SARS CoV-2 N-1 gene were used: Forward primer: 5′GAC CCCAAAATCAGCGAAAT3′ and Reverse primer: 5′ TCTGGTTACTGCCAGTTGAATCTG3′, Probe: (6-FAM/BHQ-1) ACCCCGCATTACGTTTGGTGGACC. The Ct values were used to determine viral copy numbers by generating a standard curve using a SARS CoV-2 genomic RNA standard.

Hamster lung histopathology

Lung tissue specimens from hamsters were fixed in 4% paraformaldehyde in PBS and embedded in paraffin blocks. Tissue sections of 4–6 μm thickness were stained with Hematoxylin and Eosin (H&E). Slides were examined by light microscopy for 3 histological criteria in the lung (Alveolar infiltration and exudation, vasculature inflammation and peribronchiolar infiltration with epithelial desquamation) and each criterion was scored based on the severity on a scale of 1–3 (none = 0, mild = 1, moderate = 2, severe = 3).

Flow cytometry

NALT or PLNs were harvested at necropsy along with spleens. The tissues were digested with collagenase (Sigma, C9263) and passed through 70 μm cell strainers (Corning, 431751) to prepare single cell suspensions. RBCs were lysed to remove them from spleen single cells using RBC lysis solution (BioLegend, 420302). Total cell numbers were determined by counting on a haemocytometer. To facilitate intracellular staining for cytokines, single cell suspensions were incubated for 5 h in 2 μM monensin (BioLegend, BUF074) to inhibit intracellular protein trafficking. Cells were stained with

Live/Dead Fixable Blue Dead cell stain (Invitrogen, L23105) for 10 min prior to staining with anti–CD45-BUV395 (564279), anti–CD3e-PercP-Cy5.5 (551163), anti–CD4-BV650 (563232), anti–CD8a–AlexaFluor700 (557959), and anti–CD69-FITC (557392) (all from BD Biosciences), anti–NK1.1-PE (eBioscience, 12-5941-82), and anti–γδ TCR–APC (BioLegend, 118116) for 1 h. Subsequently, cells were washed 3× with 1% BSA in PBS solution, fixed with 4% paraformaldehyde (PFA) for 20 min on ice, and permeabilised with 0.1% saponin (Sigma, 47036-50G-F) in 1% BSA in PBS solution. Intracellular staining was done for IFN-γ (anti-IFN-γ-APC-Cy7, BioLegend, 505850) and IL-17a (anti-IL-17A-BV510, BD Biosciences, 564168) for 1 h. Cells were washed 3× with 0.1% saponin in 1% BSA-PBS solution and finally resuspended in 1% BSA-PBS. Cells were acquired using a LSRFortessa cell analyzer (BD Biosciences) and analysed using FlowJo software (version 10). Heatmaps were generated using Heatmapper[46] after normalisation to saline-challenged controls and log-transformation of data.

ELISA

Recombinant S-RBD protein (Sino Biological, 40592-VOSB) was coated onto 96 well plates in carbonate (15 mM) bicarbonate (35 mM) buffer at 4 °C, overnight. Serial 2× dilutions of serum or nasal washes were added to the coated plates and incubated overnight at 4 °C. Plates were washed 3× with PBS and treated with an AP-conjugated anti-mouse IgG antibody (Southern Biotech, 1030-04) or AP-conjugated anti-mouse IgA antibody (Southern Biotech, 1040-04) for 1.5 h. For avidity ELISA, plates were washed with 4 M urea (Sigma, U5378) for 10 min prior to addition of secondary antibodies. Plates were washed again 3× with PBS and AttoPhos substrate (Promega, S1000) was added to each well. Fluorescence intensity at excitation/emission 440/560 nm was measured using a Tecan Spark 10 M plate reader after 45 min. The end-point titres were calculated at two-fold over naïve serum or naïve nasal wash on each plate.

Binding assay

The S-RBD binding antibody in mouse sera was quantified using a multiplex microsphere-immunoassay (MMIA). AviTag-enzymatic biotinylated SARS-CoV-2 ancestral, Alpha, Beta, Gamma, Delta RBDs were custom-made by Genscript. The remaining RBDs were produced in-house by transfection of pCAGGS-expression plasmids (modified from pCAG-GFP, addgene, 11150) into the Expi293F system (ThermoFisher, A14527). The RBDs were purified using Nickel Sepharose columns (Cytiva, 17526802), and biotinylated using a BirA kit (Avidity, LLC, BirA500). The RBDs were coated on the Magplex avidin-microsphere (Luminex, MA-A012-01) at 25 µg per 5 million microspheres. The RBD-coated beads were pre-incubated with 1:100 diluted mouse sera for 1 h at 37 °C with agitation at 800 rpm. Following two 1% BSA PBS washes, the mouse IgG was immunostained with 1:1000 diluted PE-labelled anti-mouse IgG antibody (R&D systems, IC002P) for 1 h at 37 °C with agitation at 800 rpm. After two washes, the MFI signals were acquired using the Luminex MAGPIX reader.

Surrogate virus neutralization assay

A study team member blinded to the experimental groups performed the multiplex sVNT assay as previously described.[47,48] In brief, serum samples at a starting dilution of 1:10 were pre-incubated with avidin microspheres coated with AviTag-biotinylated RBD proteins from different SARS-CoV-2 strains (including ancestral, Alpha, delta, Lambda, Beta, Gamma, Mu, Delta plus, Omicron BA.1 and BA.2) for 15 min at 37 °C, followed by addition of PE-labelled human ACE2 (custom made by Genescript) at a final concentration of 2,000 ng/mL for another 15 min at 37 °C. After two washes, the signals were acquired using the Luminex MAGPIX ireader.

T cell activation assay

JAWSII cells (ATCC, CRL-11904) (1.5×10^4) were seeded to each well of a 96-well flat-bottom plate in αMEM (Thermo Fisher, 22400089) with 5 ng/mL GM-CSF and incubated at 37 °C with 5% CO_2 in atmospheric air. 24 h after seeding 1 µg of S-RBD protein was added to each well. On day 3 post-seeding, spleens were harvested from vaccinated mice at day 35 post-vaccination and prepared as described above. Wells were washed with PBS and 1×10^5 splenocytes were added to each well in RPMI containing 10% FBS. Cells were incubated in a 5% CO_2 incubator at 37 °C for four days before analysis by flow cytometry. At day 7 post-seeding, cells were incubated for 5 h in 2 µM monensin to inhibit intracellular protein trafficking and then stained with Live/Dead Near IR Dead cell stain (Invitrogen, L10119) for 10 min. Cells were then stained with anti–CD3e-PercP-Cy5.5 (551163), anti–CD4-BV650 (563232), anti–CD8a–Alexa Fluor 700 (557959), anti-CD44-BV510 (563114), anti-CD62L-PE-Cy7 (560516), all from BD Biosciences and anti–CD69-eFluor450 (11-0691-82, eBioscience) for 1 h in PBS supplemented with 1% BSA on ice. Subsequently, cells were washed 3× with 1% BSA in PBS, fixed with 4% PFA at 4 °C for 20 min, and permeabilised with 0.1% Saponin in 1% BSA-PBS solution for 30 min. Intracellular staining was done for IFN-γ (anti-IFN-γ-BV711, BD Biosciences 554412) and TNFα (goat-anti-TNFα, R&D Systems AF-410-NA, anti-goat-IgG-FITC, Jackson ImmunoResearch, 305-096-006) for 1 h in permeabilisation solution. Data were acquired using LSRFortessa cell analyzer (BD Biosciences) and analysed using FlowJo software (version 10).

T cell adoptive transfer and antigen challenge

Spleens were harvested from vaccinated mice at day 35 post vaccination (with boost at day 21) and single cell suspensions were prepared as described above. RBCs were lysed using 1× RBC lysis solution and cells were counted using a haemocytometer. T cells were isolated from the splenocytes using Pan T Cell Isolation Kit II (Miltenyi Biotec, 130-095-130) according to the manufacturers protocol and 1×10^6 T cells were transferred to Thy1.1 mice by tail vein injection. Mice were challenged with 50 μg S protein (full length) I.N. in 20 μL PBS 24 h post-transfer. The SARS-CoV2 S protein was expressed using the vector pCAGGS containing the SARS-Related Coronavirus 2, Wuhan-Hu-1 Spike Glycoprotein Gene from BEI (NR-52394) and purified following the published protocol.[49] Mice were euthanised 5 days post-challenge and lungs and brachial lymph nodes were harvested. The tissues were digested with collagenase and passed through 70 μM cell strainer to prepare single cell suspensions. RBC lysis was done for spleen single cells using RBC lysis solution. Cells were stained with Live/Dead Blue Dead cell stain (Invitrogen, L23105) for 10 min. Cells were then stained with anti–CD45-BUV395 (564279), anti–CD4-BV650 (563232), anti–CD8a–Alexa Fluor 700 (557959), and anti-CD44-BV510 (563114), anti-CD62L-PE-Cy7 (560516), all from BD Biosciences, and anti–NK1.1-PE (eBioscience, 12-5941-82), anti–CD69-eFluor450 (eBioscience, 11-0691-82, or anti–CD69-PerCP-Cy5.5 45-0691-82) anti-CD90.2-PerCP-Cy5.5 (BioLegend, 140322, or anti-CD90.2-eFluor450, eBioscience, 48-0902-80) and anti–γδ TCR–APC (BioLegend, 118116). Subsequently, cells were washed, fixed with 4% PFA, and permeabilised with 0.1% Saponin in 1% BSA-PBS solution. Intracellular staining was done for IFN-γ (anti-IFN-γ-BV711, BD Biosciences 554412) and TNFα (goat-anti-TNFα, R&D Systems, AF-410-NA) in permeabilisation solution for 1 h on ice. After washing, the cells were similarly stained with secondary antibody anti-goat-IgG-FITC (Jackson ImmunoResearch, 305-096-006). Cells were acquired with a LSRFortessa cell analyzer (BD Biosciences) and analysed using FlowJo software (version 10).

Data presentation

Figures were prepared using Adobe Illustrator and diagrams were drawn using biorender.com.

Statistics

Data were analysed using Prism 9 and Microsoft Excel software. Sample size calculations were done *a priori* using data from prior vaccination studies with $\alpha = 0.05$ and $\beta = 0.8$. For multiple groups comparison, ANOVA was used, while Student's unpaired t-test was used when two groups were compared. Data were confirmed to be normally distributed prior to analysis and were log transformed to ensure a normal distribution prior to analysis, for example for analysis of antibody endpoint titers. All data are presented as the means of experimental replicates using individual mice and error bars represent the SEM throughout the manuscript. All data obtained are included in the manuscript with the exception of one flow cytometry sample that was determined to have poor cell viability by live-dead staining. No specific strategies were used to control for possible confounding factors such as order of vaccinated groups challenge.

Role of funders

The funders had no role in the study design, data collection, data analyses, interpretation, or writing of report.

Results

Superior systemic T cell responses with mucosal adjuvant

We began by comparing the ability of various vaccine formulations utilising recombinant S protein to activate T cells. For this, mice were immunised S.C. with the receptor binding domain of S protein (S-RBD), combined with either adjuvant, Alum or M7 (Fig. 1A), or I.N. with an equivalent amount of S-RBD and M7 (Fig. 1B). Although the RBD is small, our assessments suggested that there are multiple CD4 and CD8 T cell epitopes predicted for mice in this region of the S protein (Supplementary Tables S1 and S2), which is consistent with the observations in humans that the RBD contains confirmed T cell epitopes.[50] The T cell responses 5 days post-immunisation were measured by flow cytometry in the draining lymphoid organs for the respective tissues for S.C. or I.N. immunisations, respectively, either the popliteal LN (PLN) or the nasal-associated lymphoid tissue (NALT), the latter of which is the rodent structure analogous to Waldeyer's ring in humans.[51] This time point was chosen because it represents an early time following vaccination when antigen-specific CD4 and CD8 T cell responses can be detected in experimental mouse models.[52,53] Systemic T cell responses were also assessed in the spleen following either route of immunisation. The various populations of T cells found in the lymphoid organs were visualised using the UMAP algorithm (Fig. 1C) and were identified using the gating strategy shown in Fig. 1D. We first compared the numbers of total and activated T cells in these secondary lymphoid organs after subcutaneous or nasal injection with M7 + S-RBD to saline-treated or S-RBD antigen alone-treated control groups. Subcutaneous immunisations of S-RBD with M7 induced increased retention of total $CD3^+$ T cells as well as $CD8^+$ and $CD4^+$ T cell subsets in the draining PLN (Fig. 1E, Supplementary Figure S1A). Vaccination with alum + S-RBD also induced strong T cell activation responses in the local draining lymph node (Fig. 1E, Supplementary

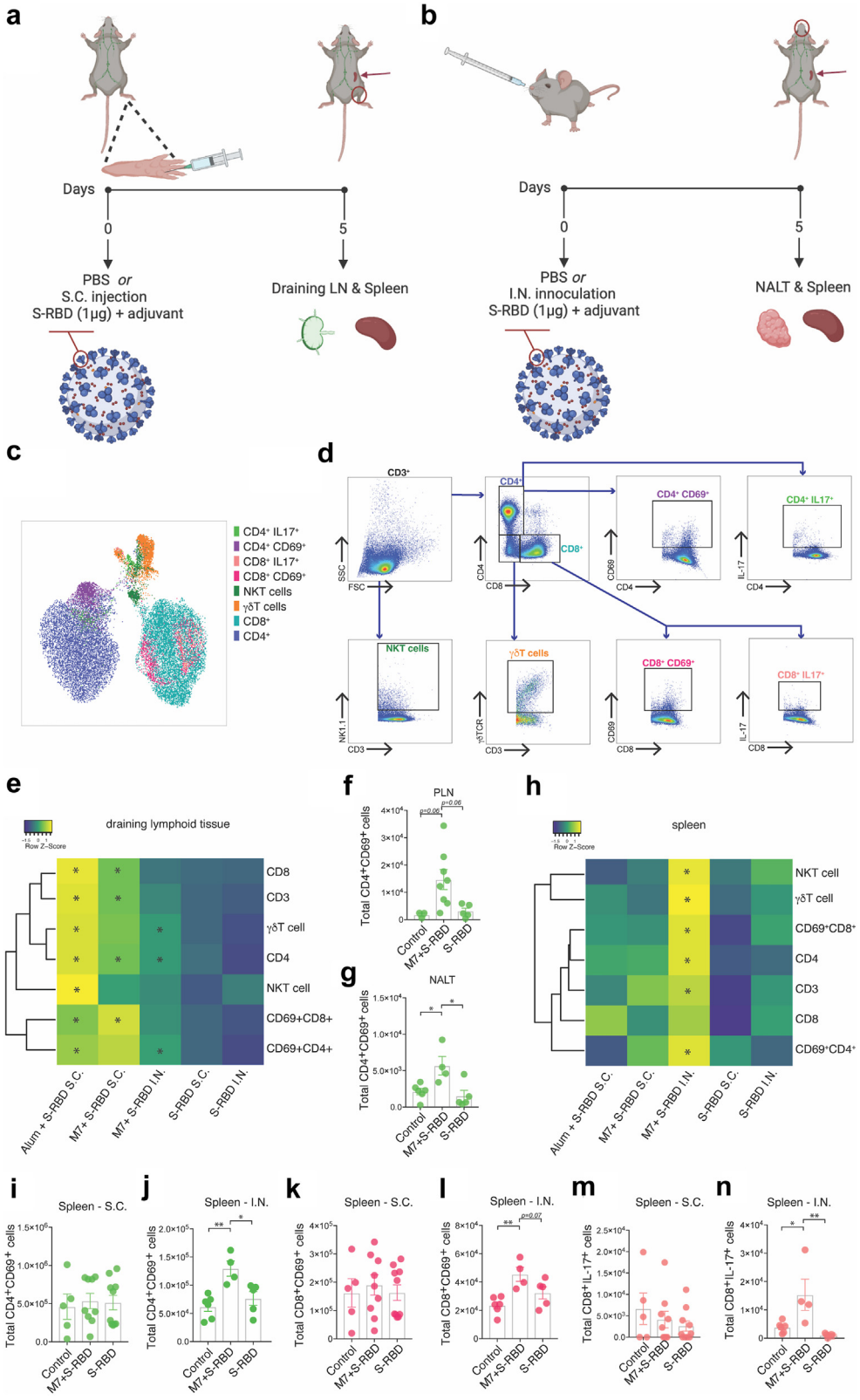
a
Days
0
5
PBS or
S.C. injection
S-RBD (1μg) + adjuvant
Draining LN & Spleen
b
Days
0
5
PBS or
I.N. innoculation
S-RBD (1μg) + adjuvant
NALT & Spleen
c
CD4+ IL17+
CD4+ CD69+
CD8+ IL17+
CD8+ CD69+
NKT cells
γδT cells
CD8+
CD4+
d
CD3+
CD4+
CD8+
CD4+ CD69+
CD4+ IL17+
NKT cells
γδT cells
CD8+ CD69+
CD8+ IL17+
e
draining lymphoid tissue
Row Z-Score
CD8
CD3
γδT cell
CD4
NKT cell
CD69+CD8+
CD69+CD4+
Alum + S-RBD S.C.
M7+ S-RBD S.C.
M7+ S-RBD I.N.
S-RBD S.C.
S-RBD I.N.
f
PLN
Total CD4+CD69+ cells
Control
M7+S-RBD
S-RBD
g
NALT
Total CD4+CD69+ cells
h
spleen
Row Z-Score
NKT cell
γδT cell
CD69+CD8+
CD4
CD3
CD8
CD69+CD4+
i
Spleen - S.C.
Total CD4+CD69+ cells
j
Spleen - I.N.
Total CD4+CD69+ cells
k
Spleen - S.C.
Total CD8+CD69+ cells
l
Spleen - I.N.
Total CD8+CD69+ cells
m
Spleen - S.C.
Total CD8+IL-17+ cells
n
Spleen - I.N.
Total CD8+IL-17+ cells

Figure S1B) and conventionally innate T cells, γδ and NKT cells were similarly increased in the PLN (Supplementary Figure S1B). In contrast, the total T cell and $CD8^+$ T cell numbers were not significantly affected in the NALT following mucosal challenge with M7 + S-RBD, while there was a small but significant increase in the total number of $CD4^+$ T cells (Fig. 1E, Supplementary Figure S1C). There were also increased numbers of activated $CD69^+CD4^+$ T cells in the NALT following I.N. vaccination, which was not observed to a significant level in the PLN after S.C. vaccination with M7 + S-RBD (Fig. 1E–G). For graphs presented in Supplementary Figure S1, corresponding cell frequencies are provided in Supplementary Table S3. These results suggest that peripheral S.C. vaccination with Alum or M7 as adjuvant results in increased activation of T cells in the PLN, while the effects of M7 on T cell activation in the NALT are more moderate and skewed towards $CD4^+$ T cell activation.

In contrast to the draining lymphoid organs, we noted that systemic activation of T cells was much higher in the spleen following mucosal vaccination. There were increased numbers of total T cells, as well as total, γδ, NKT and activated CD4 and CD8 cells after I.N. vaccination with M7 + S-RBD compared to unvaccinated or S-RBD-antigen alone treated controls, which did not occur in the S.C. vaccinated groups (Fig. 1H–L, Supplementary Figure S1D–F). These data illustrate that mucosal immunisation results in improved systemic immune activation, compared to peripheral S.C. immunisation, even comparing the same adjuvant and antigen.

In addition to T cell activation, we also measured intracellular cytokine expression in T cells, including IFN-γ, TNF and IL-17, as these cytokines define polarised T cell responses.[54] While intracellular IFN-γ and TNF were not detected at this time point, we observed $IL\text{-}17^+$ expressing $CD8^+$ T cells were uniquely enhanced in the spleen of mucosally-immunised mice, but not in the NALT of the same animals or in either the spleen or draining LNs of mice given S.C. immunisations with the same adjuvant, M7 (Fig. 1M and N). This is interesting since Th17 responses have been associated with IFN-γ-independent immune activation, augmented B cell activity, IgA induction at mucosal sites, and protective immune responses during respiratory viral infections.[55] We also observed that vaccination by both I.N. or S.C. routes and with either adjuvant, Alum or M7, and even S.C. injection of S-RBD antigen alone, promoted granzyme B expression by splenic CD8 T cells (Supplementary Figure S1G), while the numbers of IL-2 expressing CD4 T cells in the spleen were not affected (Supplementary Figure S1H). Together these results indicate that the phenotypes of T cells, and particularly their activation levels and cytokine production, are influenced by the vaccination route and adjuvant used.

Improved lung pathology in SARS-CoV-2 challenged hamsters after mucosal vaccination

To confirm that the I.N. and S.C. vaccines using M7 as an adjuvant would provide early protection from clinical disease during SARS-CoV-2 challenge, we used a previously described Syrian hamster model,[56–58] which is thought to more closely recapitulate COVID-19 disease in humans compared to mice, without the need for genetic modification.[57] Animals were vaccinated using a prime-boost strategy, followed by a challenge at 5 weeks using the Hong Kong/VM20001061/2020 virus, a parental ("Wuhan") strain virus, as shown in Fig. 2A. Although hamsters generally exhibit reduced neutralising antibody titres to S-RBD compared to other experimental model species,[59] we observed seroconversion and the presence of neutralising antibodies in all of our vaccinated animals prior to challenge (Supplementary Figure S2A). Animals were monitored daily after virus inoculation for 4 days for body mass and clinical signs and the results from vaccinated groups were compared to healthy uninfected controls and unvaccinated infected controls. Both groups of I.N. and S.C. vaccinated animals were significantly and similarly protected from

***Fig. 1:* Superior systemic T cell activation following mucosal vaccination against SARS-CoV-2.** (**a and b**) Diagrams of (**a**) sub-cutaneous (S.C.) and (**b**) intra-nasal (I.N.) vaccination strategies. (**c**) UMAP representation of the populations of T cells assessed in lymphoid organs 5 days following vaccination. (**d**) Flow cytometry gating strategy on $CD3^+$ cells to identify T cell subsets and their phenotypes and activation status corresponding to the populations depicted in panel C. (**e**) Heat map representation of the frequency of various T cell subsets day 5 following vaccination in the draining lymphoid tissue [either NALT for I.N. or popliteal LN (PLN) for S.C. vaccination]. Raw data and statistical comparisons for the M7 + S-RBD S.C. group are provided in Supplementary Figure S1A, for the Alum + S-RBD S.C. group are provided in Supplementary Figure S1B, and for the M7 + S-RBD I.N. group are provided in Supplementary Figure S1C. (**f and g**) Total activated $CD4^+CD69^+$ cells in the (**f**) PLN after S.C. M7 + S-RBD vaccination and (**g**) NALT after I.N. M7 + S-RBD vaccination. (**h**) Heat map representation of the frequency of various T cell subsets day 5 following vaccination in the spleen. (**i and j**) Numbers of $CD4^+CD69^+$ T cells in the spleen following (**i**) S.C. or (**j**) I.N. vaccination with M7 + S-RBD compared to controls or antigen (S-RBD) alone. (**k and l**) Numbers of $CD8^+CD69^+$ T cells in the spleen following (**k**) S.C. or (**l**) I.N. vaccination with M7 + S-RBD compared to controls or antigen (S-RBD) alone (**m and n**) Numbers of $IL\text{-}17^+$ CD8 T cells in the spleen following (**m**) S.C. or (**n**) I.N. vaccination with M7 + S-RBD compared to controls or antigen (S-RBD) alone. Raw data and statistical comparisons for the spleen data for the M7 + S-RBD S.C. group are provided in Supplementary Figure S1D, for the Alum + S-RBD S.C. group are provided in Supplementary Figure S1E, and for the M7 + S-RBD I.N. group are provided in Supplementary Figure S1F. N = 5–10 mice per group; $^*p < 0.05$ and $^{**}p < 0.01$ by 1-way ANOVA.

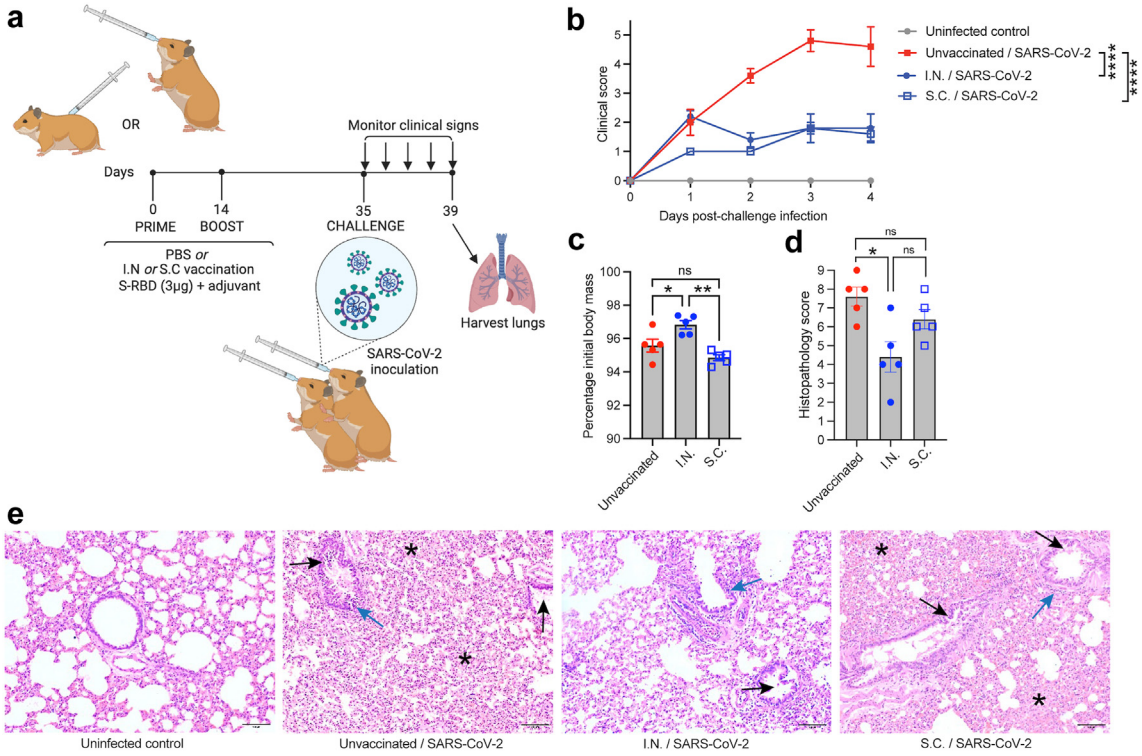

Fig. 2: **Mucosal vaccination protects hamsters from SARS-CoV-2-induced clinical disease.** (**a**) Diagram of the experimental design where hamsters were vaccinated with S-RBD and M7 via various routes using a prime (day 0) and boost (day 14). Animals were then challenged I.N. with of 10^5 plaque-forming units (PFU) SARS CoV-2 on day 35 and monitored for 4 days prior to necropsy. (**b**) Clinical scores of vaccinated animals were significantly reduced compared to unvaccinated infected controls by 2-way ANOVA with Tukey's post-test; $p < 0.0001$. n = 5 per group. (**c**) Day 4 post-infection, I.N. vaccinated animals began to recover body mass compared to unvaccinated and S.C. vaccinated controls that were also infected. *$p < 0.05$ and **$p < 0.01$ by one-way ANOVA with Tukey's post-test. (**d**) I.N. vaccinated animals had reduced lung tissue damage compared to unvaccinated animals following SARS-CoV-2 challenge, by histopathological score, determined by one-way ANOVA. $p < 0.05$. (**e**) Representative images of lung histology. Scale bar = 100 µm. Black arrows indicate examples of bronchiolar epithelial cell death and desquamation, although very mild in the I.N. group. Blue arrows indicate examples peribronchiolar cellular infiltration. Asterisks are placed to indicate examples of pronounced alveolar septal infiltration.

clinical disease compared to unvaccinated animals, based on clinical score (Fig. 2B). Although all groups of infected animals, lost weight following infection (Supplementary Figure S2B), we noted that by day 4, the final day of monitoring prior to necropsy, I.N. vaccinated animals had begun to recover their weight significantly compared to unvaccinated and S.C. vaccinated animals (Fig. 2C). However, we did not detect significant differences in virus genome quantification in the lungs at the time of necropsy (Supplementary Figure S2C), although we cannot rule out that this also relates to the early time point used following inoculation. Even so, histopathological analysis of tissues from all animals (Fig. 2D) confirmed significant protection of I.N. vaccinated animals from severe lung inflammation. I.N. vaccinated animals showed reduced peribronchiolar infiltration, vascular inflammation, and alveolar space exudation, as shown in representative images (Fig. 2E). These results support that I.N. vaccination results in protection from clinical disease compared to unvaccinated controls and while S.C. vaccination with the same formulation improved clinical scores compared to controls, the effects of vaccination on reduced histopathology compared to controls were not significant.

Improved polyfunctional memory recall by T cells upon antigen exposure following mucosal vaccination

Given the strong systemic immune response observed in the spleen immediately following mucosal vaccination of mice with M7 + S-RBD (Fig. 1H) and the improved clinical outcomes in hamsters vaccinated with the same formulation I.N. versus unvaccinated controls, which were not observed to the same significant extent in the S.C. vaccinated group versus unvaccinated controls upon SARS-CoV-2 challenge (Fig. 2C–E) we next aimed to extend beyond describing the acute T cell

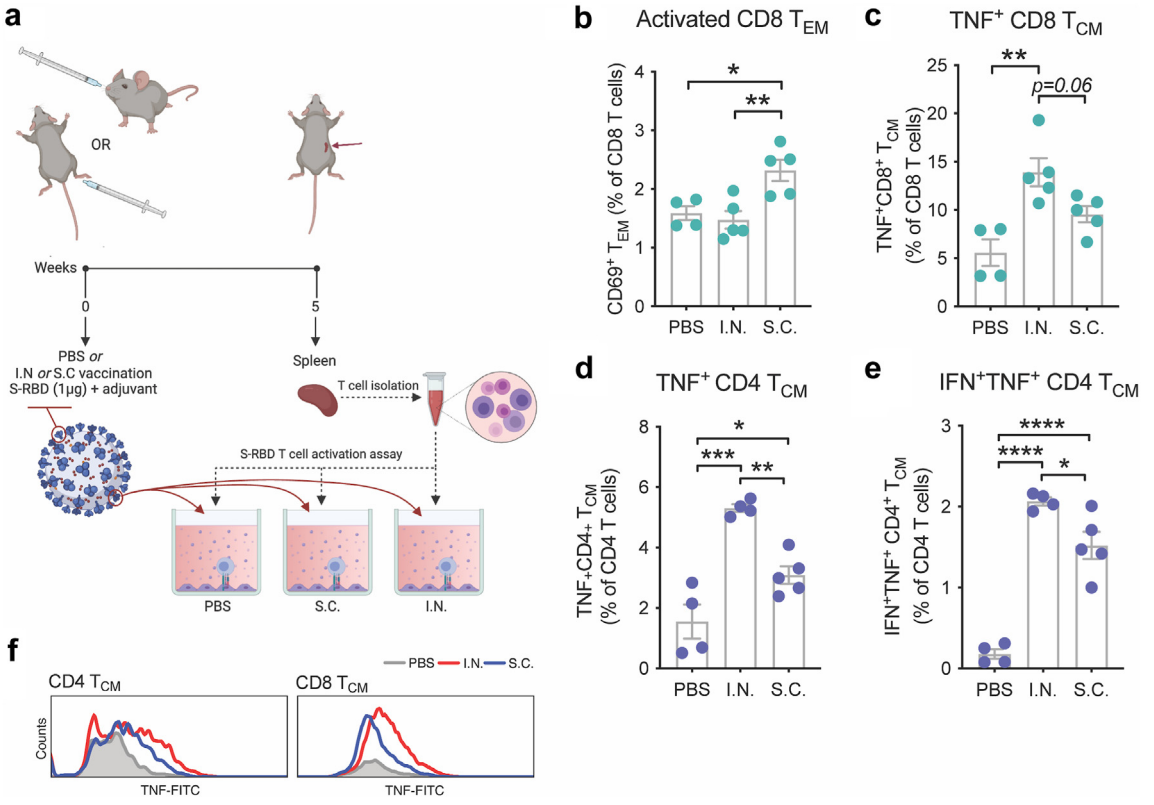

***Fig. 3:* Mucosal vaccination enhances induction of antigen-specific polyfunctional T_{CM}.** (**a**) Schematic representing the experimental design where splenocytes isolated from mice vaccinated with M7 + S-RBD by either the I.N. or S.C. route were stimulated with antigen S-RBD. (**b**) Increased activation of CD8 T_{EM} cells detected from mice vaccinated via the S.C. route, following stimulation with S-RBD. (**c**) Increased TNF^+ CD8 T_{CM} cells from mice vaccinated via the I.N. route following stimulation with S-RBD. (**d and e**) Quantification of the (**d**) TNF^+ and (**e**) IFN-γ^+TNF^+ populations of CD4 T_{CM} following antigen stimulation indicates an increase following either I.N. or S.C. vaccination compared to controls and for I.N. compared to S.C. vaccination with the same formulation of M7 + S-RBD. For (**b and c**) and (**d and e**), data points represent experimental replicates (4–5 individual mice for vaccine groups and 2 technical replicates from 2 mice for PBS group). (**f**) Representative histograms showing strong induction of TNF following I.N. compared to S.C. vaccination after antigen (S-RBD) stimulation. *p < 0.05, **p < 0.01, ***p < 0.001, ****p < 0.0001 by 1-way ANOVA with Tukey's post-test.

responses elicited by the vaccine by comparing the antigen-specific T cell memory responses. For this, we returned to the mouse model to allow further immunological characterisation and T cells were harvested from spleens 5-weeks post-vaccination for mice given S.C. versus I.N. challenges with the same antigen and adjuvant combination (M7 + S-RBD) and tested *ex vivo* for their activation following antigen stimulation, according to the experimental design shown in Fig. 3A. Memory T cell (T_{MEM}) populations were identified with the gating strategy provided in Supplementary Figure S3A. Antigen stimulation induced expansion and activation of CD4 and CD8 T effector memory (T_{EM}) and T central memory (T_{CM}) cells in vaccinated groups over the baseline found in naïve animals, but there were not significant differences in these populations between the two routes of vaccine administration (Supplementary Figure S3B–H), except for the elevated numbers of activated CD8 T_{EM} cells, based on CD69 expression, observed in the S.C. group (Fig. 3B). This seemed consistent with the strong induction of CD8 T cells at day 5 following S.C. immunisation (Fig. 1E). Intracellular staining for cytokines identified a heightened functional response by both CD4 and CD8 T_{CM} cells, where a higher proportion of T_{CM} cells were TNF^+ following I.N. compared to S.C. immunisation (Fig. 3C and D). Furthermore, I.N. immunisation induced more CD4 T_{CM} cells that were polyfunctional based on the co-expression of TNF and IFN-γ (Fig. 3E, Supplementary Figure S3I). Not only were the proportions of TNF^+ T_{CM} cells higher following antigen stimulation of T cells from I.N. compared to S.C. vaccine groups, but higher expression of TNF was also apparent by flow cytometry (Fig. 3F). Stronger T_{CM} functional responses after I.N. vaccine administration is consistent with increased activity of memory cells that

are able to home to multiple LNs by virtue of their CD62L expression.[60] These results support that, even controlling for vaccine formulation by using the same adjuvant, mucosal immunisation promotes greater systemic antigen-specific memory responses compared to S.C. injection, where the response is concentrated in the draining LNs. Furthermore, recall of those T_{MEM} cells from I.N. vaccination leads to an enhanced polyfunctional phenotype based on the expression of multiple cytokines.

We next questioned whether the improved polyfunctional T cell phenotype induced by mucosal vaccination was T cell-intrinsic and if it would influence immune responses in the lung upon antigen challenge. To address this question, we performed an adoptive transfer experiment using the Thy1.1/1.2 system for tracking donor versus recipient T cells (Fig. 4A). For this, T cells were harvested from the spleens of Thy1.2$^+$ mice given I.N. or S.C. vaccination with M7 + S-RBD, with a boost to ensure robust responses, and adoptively transferred into recipient mice with Thy 1.1$^+$ T cells. To simulate a viral infection without the potential of differential viral replication kinetics influencing the T cell recruitment and activation, mice were given an I.N. challenge of full-length S protein. After allowing 5 days for memory recall and CD8 T cell trafficking, we isolated the lungs and their draining LNs, the brachial LNs, to assess the phenotypes and activation profiles of donor Thy1.2$^+$ T cells (Fig. 4A, gating strategy in Supplementary Figure S4A). As expected, Thy1.2$^+$ donor T cells from vaccinated groups could be detected in the lungs of Thy1.1$^+$ recipient mice following S-antigen challenge (Fig. 4B) and these were mostly CD8 T cells (Fig. 4C), whereas CD4 cells in the lungs had very low frequency (Supplementary Figure S4B). Neither unvaccinated control mice nor vaccinated control mice given S-antigen challenge exhibited T cell recruitment to the lungs, suggesting the antigen-specificity of the response in mice given T cells from vaccinees (Fig. 4B). Given the scarcity of donor CD4 T cells in lungs and based on the important functions of CD8 T cells in responding to viral infections in peripheral tissues, we focused on characterising donor memory CD8 T cells. First, we noted there were no significant differences in the numbers of memory CD8 T cells that were recruited into the lung tissue between groups whose donor T cells were derived from I.N. versus S.C. vaccinated animals (Fig. 4C). However, we observed that donor memory CD8 T cells expressed higher levels of TNF compared to recipient memory CD8 T cells for both vaccination groups, with the highest levels expressed in the group having donor T cells from mice with I.N. vaccination (Fig. 4D), suggesting improved antigen-specific activation at the challenge site. The donor memory CD8 T cells in the lungs also expressed higher levels of TNF as determined by MFI of flow cytometry (Fig. 4E) and, interestingly they also expressed higher levels of the activation marker CD69 by MFI (Fig. 4F). These results suggest that while there was no effect on the efficiency of memory CD8 T cell recruitment into the lungs following challenge, the T_{MEM} cells from I.N. vaccinated mice were more activated and functional following their entry into the lung tissue, supporting improved antigen-specific recall.

We also questioned whether S antigen challenge in animals (as performed in Fig. 4A) would induce heightened T_{CM} responses and polyfunctional T cell responses *in vivo* in lung draining LNs following transfer of T cells from I.N. compared to S.C. challenges, similar to our observations in *ex vivo* assays (Fig. 3). Donor T cells could be identified in the brachial LNs based on Thy1.2 expression (Fig. 5A and B, Supplementary Figure S4C). We examined the CD4 and CD8 subsets of memory donor T cells and noted the presence of both CD4 and CD8 populations that expressed cytokines including TNF and IFN-γ (Fig. 5B and C, Supplementary Figure S4D and E) which were more abundantly present in the LNs of mice that received donor T cells from vaccinated mice (Fig. 5C). Additionally, significantly increased proportions of donor CD8 T cells having the T_{CM} and T_{EM} phenotypes were present in brachial LNs for the I.N. vaccinated group (Fig. 5C–E). Furthermore, more CD8$^+$ and CD4$^+$ donor memory cells in the brachial LN produced cytokines TNF and IFN-γ following antigen challenge in mice receiving T cells derived from I.N. vaccination compared to S.C. vaccination (Fig. 5F and G). These results indicate that T cells develop an improved polyfunctional phenotype following I.N. vaccination, able to respond to challenge in the lung-draining LNs with higher levels of activation and cytokine production.

Superior antibody responses and clinical protection following mucosal vaccination

We identified improved systemic T cell responses following I.N. compared to peripheral S.C. vaccination; however, given the high correlation between antibody responses and protection against symptomatic infection for humans vaccinated against SARS-CoV-2,[16] we also questioned whether mucosal vaccination influenced antibody responses. Mucosal vaccination is associated with improved IgA responses,[33] and consistent with this we observed that I.N. vaccination improved Spike-specific IgA secretion in nasal washes, compared to S.C. vaccination with the same formulation by ELISA (Fig. 6A). Moreover, we were also curious if there were differences in antibody specificity and neutralising ability resulting from the different vaccination routes. Therefore, we also characterised serum IgG responses against S-RBD. Early responses at 3 weeks post-immunisation showed no difference in binding to the same antigen, S-RBD, between mice exposed to the M7-S-RBD vaccine via the I.N. or S.C. routes; however, by 5 weeks post-immunisation, anti-S-RBD titres were

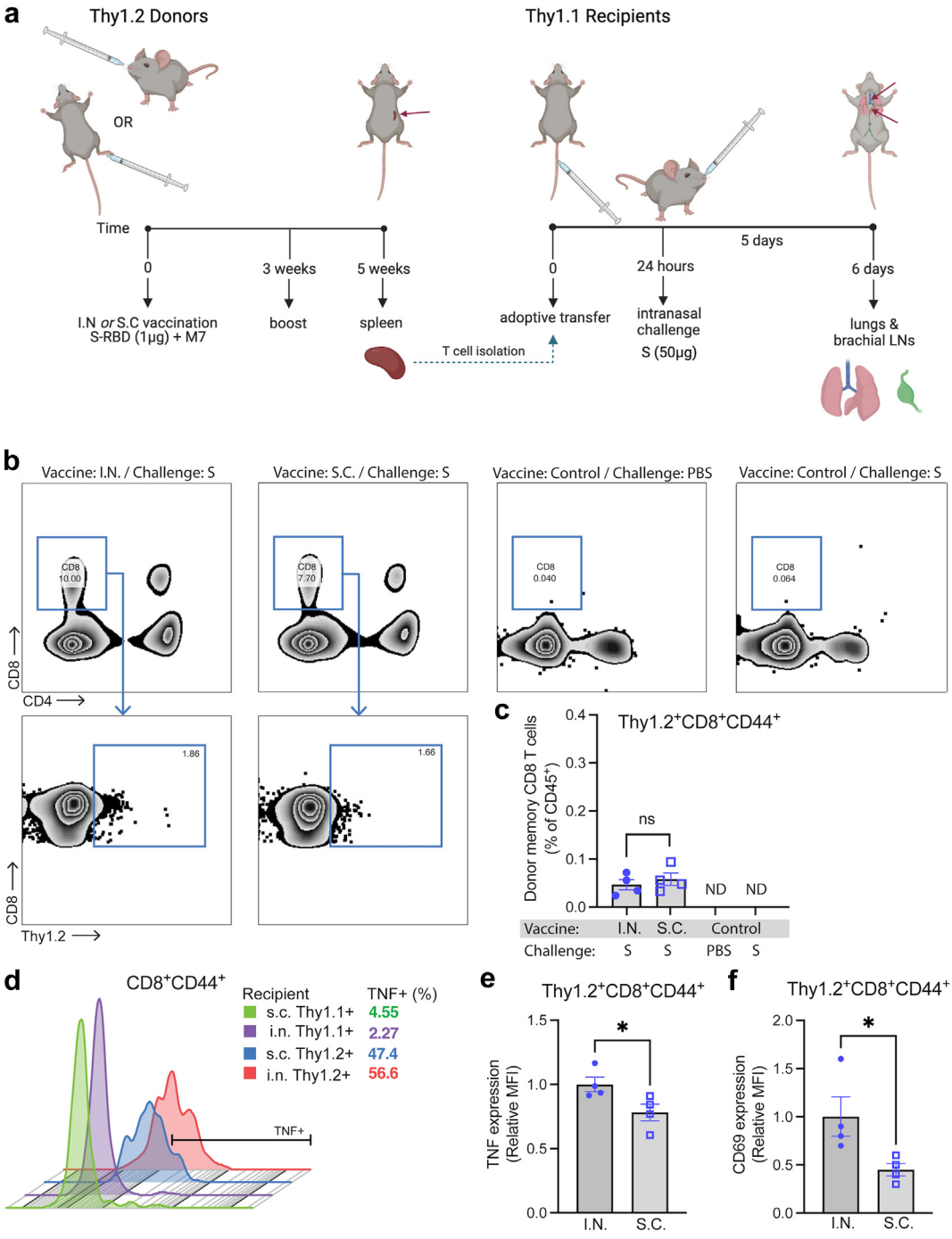

Fig. 4: **Improved re-activation of memory T cells derived from I.N. vaccinated donors in recipient lungs upon challenge.** (**a**) Diagram illustrating the experimental design of adoptive transfer of purified Thy1.2$^+$ T cells from M7 + S-RBD-vaccinated donors (via S.C. or I.N. routes) into Thy1.1$^+$ naïve recipients, followed by I.N. challenge with S protein. (**b**) Flow cytometry plots indicating the presence of donor Thy1.2$^+$CD8$^+$ T cells in the lungs of vaccinated recipient mice, but not control mice, 5 days after challenge. Full gating strategy provided in Supplementary Figure S4A. (**c**) Donor Thy1.2$^+$CD8$^+$ T cells constituted a minor portion of haemopoietic cells in the lung following challenge and did not differ in frequency between I.N. or S.C. vaccinated groups, but were not detected in control mice. (**d**) Histogram of TNF expression on donor (Thy1.2$^+$) and recipient (Thy1.1$^+$) CD44$^+$CD8$^+$ T cells representative of each group indicates an increase in TNF expression by donor T cells in lungs from vaccinated mice. Downsampling of 600 T cells was used to facilitate comparisons of equal numbers of cells for each sample. The percentage of TNF$^+$ cells of total CD44$^+$CD8$^+$ T cells is indicated in the legend. (**e and f**) The MFI for (**e**) TNF expression and (**f**) CD69 expression were

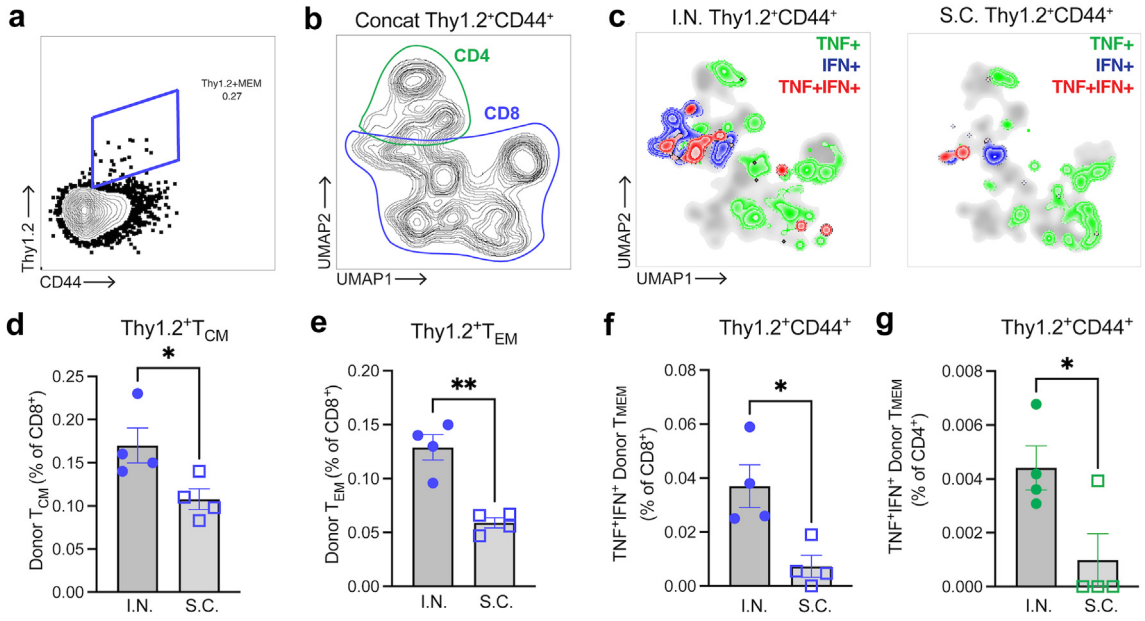

Fig. 5: **Mucosal vaccination enhances memory T cell responses in brachial LNs.** (**a**) Identification of donor Thy1.2$^+$ T_{MEM} cells and (**b**) UMAP presentation (concatenated representation of all groups) with the locations of CD4 and CD8 T cell subsets outlined on the plot. Full gating strategy is provided in Supplementary Figure S4C. (**c**) Donor T_{MEM} cells (Thy1.2$^+$CD44$^+$) expressing the cytokines TNF and/or IFN-γ are shown by overlaying the cytokine-positive subpopulations over the total UMAP plots for each group I.N. (left) versus S.C. (right). All samples from each experimental or control group (n = 4 mice) are concatenated to generate the respective plots. (**d and e**) Plots indicating the percentage of donor-derived CD8 T cells with the (**d**) T_{CM} or (**e**) T_{EM} phenotypes. Percentage of (**f**) CD8 and (**g**) CD4 T cells that are donor T_{MEM} cells, staining double-positive for cytokines (TNF$^+$IFN-γ$^+$). N = 4–5 mice per group derived from two independent experiments *p < 0.05, **p < 0.01 by Student's unpaired t-test.

significantly higher in mice vaccinated via the mucosal I.N. route (Fig. 6B). No significant differences in antibody avidity were observed to the same S-RBD used as the vaccine antigen (Fig. 6C), suggesting the polyclonal antibodies had a similar polyclonal strength of binding to the original antigen used for vaccination. We also wanted to gain an understanding of whether the antibodies induced could be protective against SARS-CoV-2 and, therefore, used a surrogate virus neutralization test which detects total immunodominant neutralising antibodies targeting S-RBD.[47] The surrogate neutralization test against S-RBD from an ancestral strain similar to the antigen used for vaccination, the Singapore/2/2020 strain, revealed that there was effective and similar concentration-dependent induction of neutralising antibodies by both I.N. and S.C. vaccination routes (Fig. 6D). We also investigated the potential of antibodies generated by I.N. versus S.C. vaccine exposure to induce antibodies with cross-neutralising capacity towards other variants of SARS-CoV-2. While S.C. inoculation induced efficient neutralising antibodies against the Alpha variant in addition to the parental strain, cross-neutralization against other variants tested was low for the Delta, Delta plus, and Gamma VOCs and not significantly present for others (Fig. 6E, Supplementary Figure S5). In contrast, I.N. vaccination induced more broadly cross-protective antibodies, with more significant neutralization at higher dilutions, which was significant compared to naïve controls for all variants tested, including Alpha, Delta, Beta, Gamma, Delta plus, Lambda, Mu, OmicronBA.1, and OmicronBA.2 (Fig. 6E, Supplementary Figure S5). This increased neutralization was not associated with any significant differences in antibody binding to the S-RBD of each variant by vaccination group (Fig. 6F). Indeed, antigen binding for each variant was not significantly correlated with sVNT titre, and a shift could be seen indicating more efficient neutralization of VOC by sera from I.N. vaccinated animals at these similar binding titres to S.C. vaccinated groups (Fig. 6G). This suggests that mucosal vaccination alters the breadth of neutralising antibodies and may promote broadly neutralising responses.

compared for Thy1.2$^+$ donor CD8 T_{MEM} cells in the lungs following S challenge. For (**e and f**), vaccinated groups were not compared to control groups since there were insufficient donor memory T cells in the lungs of unvaccinated control groups for TNF expression quantification. N = 4–5 mice per group derived from two independent experiments. *p < 0.05 by Student's unpaired t-test.

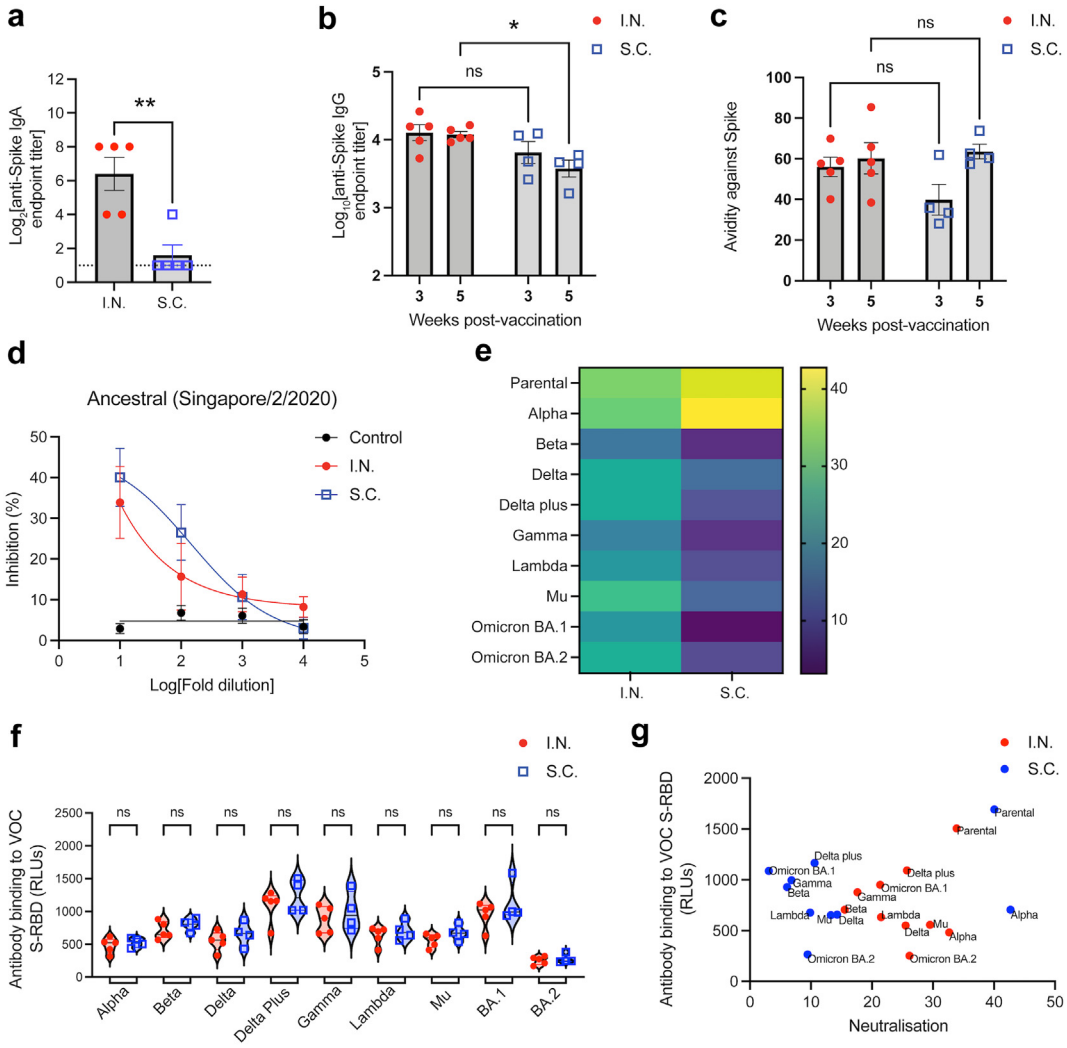

Fig. 6: **Superior antibody titre and SARS-CoV-2 variant cross-neutralisation after mucosal vaccination.** (**a**) Anti-S-RBD IgA endpoint titres in nasal washes, 21 days post-immunisation. (**b and c**) Serum Anti-S-RBD IgG (**b**) endpoint titres and (**c**) avidity (percentage serum antibody that remains bound after stringent ELISA washing) following S.C. or I.N. vaccination. *p < 0.05, by two-way ANOVA. ns = not significant. (**d**) Percentage inhibition of S-RBD association with its receptor hACE-2 by serum antibodies, determined by s-VNT. For control versus I.N, p = 0.003; for control versus S.C. p < 0.001. For I.N. versus S.C., the comparison was not significantly different. (**e**) Heatmap depicting the % inhibition against S-RBD from multiple SARS-CoV-2 variants at 1:10 serum dilution. Corresponding dose response curves with p-values are provided in panel (**d**) and Supplementary Figure S5. (**f**) Comparison of serum antibody binding to S-RBD from multiple VOC between the I.N. and S.C. vaccination groups, determined by ELISA. RLU = relative light units. (**g**). No correlation between antigen binding and neutralisation (by sVNT) was observed.

Given the unique profile of T cell and antibody responses following mucosal vaccination in mice and the suggestion that VOC may be better cross-neutralized by antibodies elicited by mucosal vaccination, we also questioned whether VOC cross-protection would be observed in the hamster challenge model. Using the same experimental time course in Fig. 2A, we vaccinated hamsters using the same parental strain S-RBD antigen but challenged them with a virulent isolate of the Omicron VOC (USA/PHC658/2021). As observed for the homologous challenge (Fig. 2), we did not observe any changes in lung viral titres on day 4 at the time of necropsy (Supplementary Figure S6A), but at the same time point protection from clinical disease was observed in both vaccinated groups since only the unvaccinated, Omicron-infected group still had a significantly increased clinical score above baseline (Fig. 7A). Consistent with observations in humans,[61,62] the disease induced by Omicron was more mild than the disease induced by the parental strain (Hong Kong isolate)

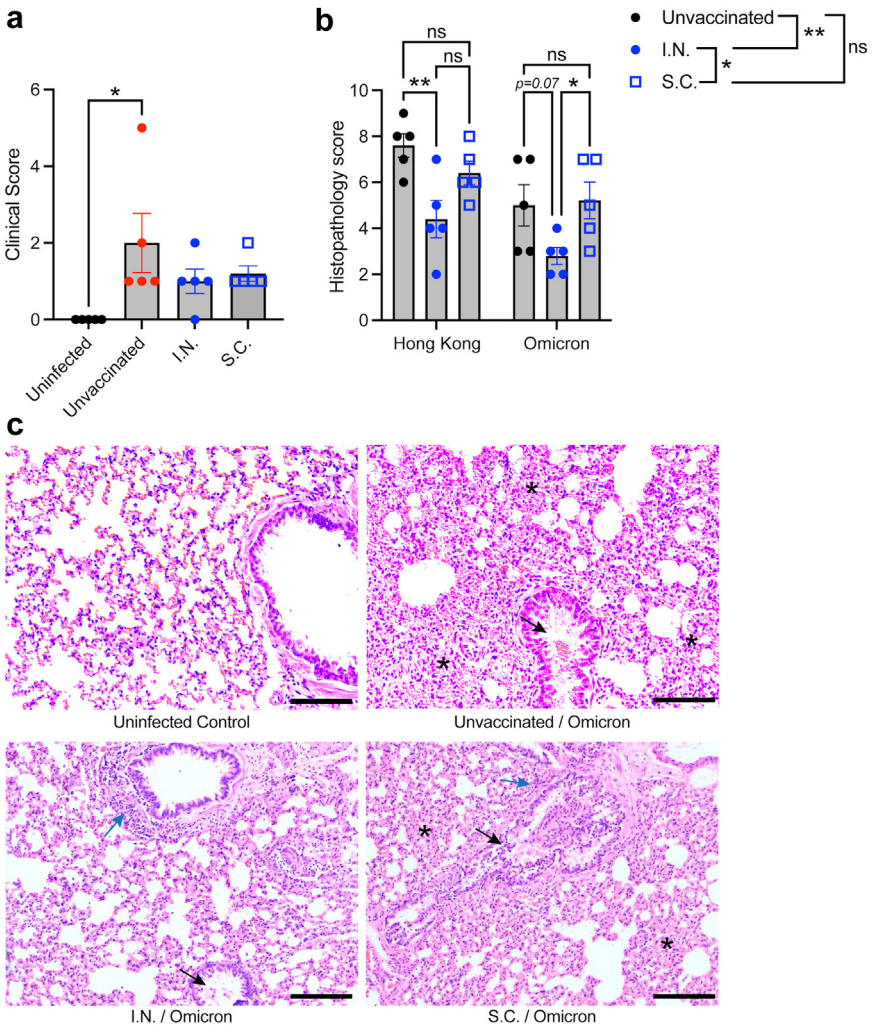

Fig. 7: **Improved lung histopathological scores for I.N. vaccinated hamsters during a heterologous challenge with Omicron.** Groups of vaccinated and unvaccinated hamsters (n = 5) were challenged with 10^5 PFU of Omicron VOC (USA/PHC658/2021). (**a**) Elevated clinical scores day 4 post-Omicron challenge in unvaccinated animals compared to uninfected controls. *p < 0.05 by 1-way ANOVA with Tukey's post-test. (**b**) Comparison of histopathological scores for Hong Kong (parental strain, Hong Kong/VM20001061/2020) and Omicron-challenged hamsters. Data from Hong Kong challenged hamsters is re-presented from Fig. 2 to aid comparison. Comparisons of individual vaccine groups for each challenge are indicated on the graphs and comparisons of the influence of vaccination group, independent of the virus challenge strain, are indicated on the figure legend. **p < 0.01 and *p < 0.05 by two-way ANOVA with Tukey's post-test. The virus strain accounted for 19.7% (p = 0.0034) of the variation in the data, while 33.5% of the variation was accounted for by the vaccination group (p = 0.0012). (**c**) Representative images of lung tissue from Omicron-infected hamsters, day 4 post-infection. Scale bar = 100 µm. Black arrows indicate examples of bronchiolar epithelial cell death and desquamation, although very mild in the I.N. group. Blue arrows indicate examples peribronchiolar cellular infiltration. Asterisks are placed to indicate examples of pronounced alveolar septal infiltration.

based on the clinical score (Figs. 2B and 7A, and Supplementary Figure S6B showing the comparison). As with the parental strain challenge (Hong Kong), we also observed reduced pathology in the lungs of hamsters in the I.N. vaccinated group (Fig. 7B), particularly with respect to reduced infiltration of cells into the lung tissue and reduced oedema in alveolar spaces compared to unvaccinated animals (Fig. 7C), which was also significantly lower than the S.C. vaccinated group by histopathological score (Fig. 7B). These data support that there are subtle but quantitative improvements to cross-protection from disease induced by mucosal vaccination.

Discussion

Mucosal vaccination has been increasingly acknowledged as a promising strategy to improve next-generation COVID-19 vaccine efficacy and immune

protection of the airways.[39,63–68] Here we tested vaccine formulations for I.N. versus S.C. delivered S-RBD antigen, combined with mucosal adjuvant M7, and showed significant protection of SARS-CoV-2-infected hamsters from clinical disease. While it is possible that the significantly reduced lung pathology, compared to unvaccinated controls, observed in animals that had been given I.N. vaccination was the effect of the improved IgA secretion that results from I.N. vaccination, we also observed distinct effects of mucosal vaccination on T cell and IgG responses. We show that mucosal vaccination against S-RBD antigen of SARS-CoV-2 promotes a T cell-intrinsic phenotype that is associated with superior systemic immune responses and antibody responses that result in improved antibody persistence *in vivo* in mice and cross-neutralization against SARS-CoV-2 variants compared to S.C. vaccination with the same formulation.

We observed heighted systemic T cell responses in multiple T cell subsets in the spleen during the acute activation phase following mucosal vaccination, which also persisted in the T_{MEM} cell compartment several weeks following challenge. T_{MEM} cells generated by mucosal vaccination also exhibited an improved polyfunctional phenotype, characterised by dual expression of TNF and IFN-γ, both upon *ex vivo* stimulation as well as during *in vivo* memory recall to antigen. *In vivo* splenic T cell responses during the acute phase following vaccination were also characterised by improved IL-17 production and heightened granzyme B expression. Granzyme B induction has been associated with the Th0 to Th1 transition.[69] Interestingly, IL-17 has been associated with lung IgA secretion,[70] which we also observed was improved in our mice following mucosal vaccination. Adoptive transfer of T cells obtained after resolution and contraction of the vaccine-induced response from vaccine recipients who had been given the exact same formulation of antigen and adjuvant, differing only by site of inoculation, confirmed the T cell-intrinsic imprinting of the site of inoculation on the T_{MEM} phenotype. Interestingly, respiratory viral infections are thought to induce CD8 T cells that have improved lung-homing capabilities.[71] Importantly, in our study, improved T cell activation and polyfunctionality in the lungs following antigen-challenge occurred in recipient mice who had been transferred T cells from I.N. rather than S.C. vaccination. This occurred even though similar numbers of T cells were recruited into the lung tissue for both recipient groups. Consistent with our study, others have also observed robust T cell activation following mucosal vaccination in animal models of subunit vaccination with S protein.[43] Our work illustrates that the polyfunctional nature of T_{MEM} cells, independent of their peripheral tissue homing abilities, could contribute to mucosal site protection. These data also highlight the role of T cells in establishing systemic mucosal vaccine-induced memory since these responses can be adoptively transferred by T cells. A goal of vaccination is to induce the type of immune response that most closely approximates natural immune protection against infection, while eliminating risks of disease. For COVID-19, despite some controversy,[72] human vaccinees to parental SARS-CoV-2 do not appear to induce robust airway-resident antigen-specific T cells, unlike those who experienced natural infections.[73,74] This highlights the potential of next-generation COVID-19 vaccines to improve mucosal and systemic immune responses through modulation of T cells.

Of the T_{MEM} cells affected by our vaccination strategy, we identified that T_{CM} cells are a central component of systemic mucosal vaccine-induced immunity. Activated and/or polyfunctional T_{CM} cells were observed in the spleen following vaccination, as well as in the T_{MEM} compartment that was effectively recalled by antigen restimulation. While antigen-specific T_{CM} were also present in subjects that received S.C. administered vaccine, and they could also be reactivated following adoptive transfer, as expected, both their numbers and the magnitude of their cytokine production responses were heightened in mucosal vaccinees. T_{CM} cells are particularly defined by their expression of CD62L, which allows them to roll on high endothelial venules and enter secondary lymphoid tissues.[75] It is likely that the increased numbers of CD62L-expressing cells within the T_{MEM} compartment following mucosal vaccination is key for the homing of these cells to the spleen that typifies increased systemic immunity. These results were observed in the context of antigen delivery with an appropriate mucosal adjuvant, while equivalent concentrations of antigen alone induced sub-optimal T cell activation responses. Efficient conversion to the T_{CM} phenotype could allow broader dissemination of antigen-specific T_{MEM} cells, which could increase the chances of subsequent exposure to antigen and memory recall and/or potential to provide B cell help in other lymphoid organs. During memory recall, T_{CM} are also thought to serve as a pool of T cells that can replenish the T_{EM} population.[76–79] Consistent with this, *in vivo* antigen challenge was also associated with significantly increased numbers of CD8 T_{EM} cells in the lung-draining brachial LNs of recipients of T cells from I.N. vaccinated groups, even though *ex vivo* antigen restimulation of spleen T cells prior to transfer resulted in improved activation for CD8 T_{EM} in the S.C. vaccinated group. These results highlight the potential of site-specific immune responses to influence the balance and tissue homing abilities of T_{MEM} sub-populations.

Systemic T cell responses are also likely to impact B cell-dependent antibody responses, owing to the influence of T cells, particularly CD4 T cells, on B cell help and germinal centre activity.[80,81] A subset of CD4 T_{CM}

expressing CXCR5 are also highly consequential to germinal centre production since they can upregulate BCL-6 during memory recall, promote plasma cell differentiation and drive secondary germinal centre formation and antibody production.[82–85] Consistent with this, we have identified improved antibody responses that coincide with the characterisation of mucosal vaccine-induced responses as dominated by polyfunctional T_{CM}. Both S.C. and I.N. vaccination strategies induced S-specific antibodies of similar avidity and neutralization towards the parental S protein, yet differences in antibody responses were also significant. I.N. vaccination induced a small but significantly higher level of antibodies at 5 weeks after the final vaccine boost and more broadly neutralising antibodies against multiple VOC, compared to S.C. vaccination. Often, we assume that mucosal vaccination influences antibodies primarily through inducing IgA secretion,[33] and here too we observe antigen-specific IgA production was uniquely induced by the I.N. challenge model. However, our data also emphasise that gains in serum IgG quality could be, at least in certain contexts, an additional benefit to mucosal vaccination. Since broadly-neutralising antibody responses were induced without altered avidity and without changes in antibody binding to the same S-RBD antigens from multiple VOC, this suggests that the mucosal vaccination strategy might have resulted in the preservation of antibodies against more diverse epitopes within the polyclonal pool.

Our results here are unique in that we are able to directly compare the responses induced by the same dose of antigen for two routes of immunisation as M7 adjuvant is effective as an adjuvant both when injected in the skin and also when administered at mucosal surfaces. However, the limitations of S.C. vaccination were not the result of the adjuvant alone, as M7 has been shown to perform well as an adjuvant when injected S.C.,[35,37] and these differences were also consistently observed when compared to the human-approved adjuvant, Alum. Even so, it is also possible that some of the vaccine-induced effects observed here are adjuvant specific, since the adjuvant's mechanism of mast cell activation (likely with some other beneficial effects on other myeloid cells[86]) is unique compared to other strategies, and since mast cell phenotypes in these tissues are different.[87] We also observed that both vaccine routes could limit clinical disease during a subsequent virulent challenge in hamsters, which emphasises that significant differences in immune responses may not always convert to unique and enhanced protective capacity. Although we did not observe a significant reduction in viral genome copies in this model, it is possible that the infection clearance kinetics could differ at later time points and that the 4 day time point was too early to observe differences in viral clearance. However, humans that are given Spike protein-based vaccines also appear to have significantly reduced risk of severe disease,[88,89] while viral burden in the nasal passages appears similar between the vaccinated and unvaccinated in many studies,[90,91] although not all.[92–94] This also supports that protection from clinical disease could be linked to the phenotype of vaccine-induced immune responses. Here, we have exposed hamsters to the live SARS-CoV-2 challenge 5 weeks following vaccination, which models the immediate host responses to vaccines. Future studies will be needed to determine if the host responses remain equally durable by both routes of immunisation and if the improved systemic T_{CM} activation and VOC cross-neutralising antibodies function to improve responses during subsequent challenges, which in humans, unlike laboratory animals, could occur many years following vaccination.

Improved systemic immune responses and improved variant cross-neutralising antibodies generated by mucosal vaccination could be applied to next generation vaccines against SARS-CoV-2 and other respiratory pathogens. Indeed, the current situation where vaccines rely on high titre specific neutralising antibodies with limited induction of mucosal responses has room for improvements. Strategies of vaccination against SARS-CoV-2 with improved capacity to limit vaccine breakthrough infections and to reduce transmission are still needed and this study and others support that mucosal vaccination is a promising strategy to meet these goals.

Contributors

Experiments were performed by AO, CKM, TCW, WAAS, SKN, MPK, and CMJ. Hamster studies were conducted by SKN, CMJ and ST. LFW and TCW developed the sVNT assay and contributed to data interpretation. Experiments were designed primarily by AO, APSR, ST, and ALS, with contributions by all authors. The underlying data were verified by ALS and AO or CKM (flow cytometry data), WAAS (serology data), TCW (sVNT data), or SKN, CMJ, and ST (hamster challenge data). The manuscript was written by ALS. All authors contributed to discussions and editing of the manuscript. All authors read and approved the final version of the manuscript.

Data sharing statement

All data are included in the manuscript. Additional supporting data are available from the authors upon request.

Declaration of interests

ALS is an inventor on a patent relating to mucosal vaccination against COVID-19. LFW and TCW are co-inventors on a patent for the sVNT assay and receive royalties from the cPass kit.

Acknowledgements

The authors thank Antonio Bertoletti for insightful discussions. This study was funded by Duke-NUS start-up funding and Singapore Ministry of Education funding to ALS (MOE-T2EP30120-0011, T2EP30222-0017) and National Medical Research Council funding to LFW (STPRG-FY19-001, COVID19RF-003, COVID19RF-060 and OFLCG19May-0034) and a DBT-BIRAC Grant (BT/CS0007/CS/02/20) to ST.

Appendix A. Supplementary data

Supplementary data related to this article can be found at https://doi.org/10.1016/j.ebiom.2023.104924.

References

1 Huang C, Wang Y, Li X, et al. Clinical features of patients infected with 2019 novel coronavirus in Wuhan, China. *Lancet*. 2020;395(10223):497–506.
2 St John AL, Rathore APS. Early insights into immune responses during COVID-19. *J Immunol*. 2020;205(3):555–564.
3 Wool GD, Miller JL. The impact of COVID-19 disease on platelets and coagulation. *Pathobiology*. 2021;88(1):15–27.
4 Li Q, Guan X, Wu P, et al. Early transmission dynamics in Wuhan, China, of novel coronavirus-infected pneumonia. *N Engl J Med*. 2020;382:1199–1207.
5 Munro APS, Janani L, Cornelius V, et al. Safety and immunogenicity of seven COVID-19 vaccines as a third dose (booster) following two doses of ChAdOx1 nCov-19 or BNT162b2 in the UK (COV-BOOST): a blinded, multicentre, randomised, controlled, phase 2 trial. *Lancet*. 2021;398(10318):2258–2276.
6 Falsey AR, Sobieszczyk ME, Hirsch I, et al. Phase 3 safety and efficacy of AZD1222 (ChAdOx1 nCoV-19) Covid-19 vaccine. *N Engl J Med*. 2021;385(25):2348–2360.
7 Baden LR, El Sahly HM, Essink B, et al. Efficacy and safety of the mRNA-1273 SARS-CoV-2 vaccine. *N Engl J Med*. 2021;384(5):403–416.
8 Thomas SJ, Moreira ED Jr, Kitchin N, et al. Safety and efficacy of the BNT162b2 mRNA Covid-19 vaccine through 6 months. *N Engl J Med*. 2021;385(19):1761–1773.
9 *COVID-19 vaccines*. Bethesda (MD): Drugs and Lactation Database (LactMed); 2006.
10 Lipsitch M, Krammer F, Regev-Yochay G, Lustig Y, Balicer RD. SARS-CoV-2 breakthrough infections in vaccinated individuals: measurement, causes and impact. *Nat Rev Immunol*. 2022;22(1):57–65.
11 Mistry P, Barmania F, Mellet J, et al. SARS-CoV-2 variants, vaccines, and host immunity. *Front Immunol*. 2021;12:809244.
12 Polack FP, Thomas SJ, Kitchin N, et al. Safety and efficacy of the BNT162b2 mRNA Covid-19 vaccine. *N Engl J Med*. 2020;383(27):2603–2615.
13 Zhou P, Yang XL, Wang XG, et al. A pneumonia outbreak associated with a new coronavirus of probable bat origin. *Nature*. 2020;579:270–273.
14 Xu X, Chen P, Wang J, et al. Evolution of the novel coronavirus from the ongoing Wuhan outbreak and modeling of its spike protein for risk of human transmission. *Sci China Life Sci*. 2020;63(3):457–460.
15 Zhao Y, Zhao Z, Wang Y, Zhou Y, Ma Y, Zuo W. Single-cell RNA expression profiling of ACE2, the receptor of SARS-CoV-2. *Am J Respir Crit Care Med*. 2020;202(5):756–759.
16 Goldblatt D, Alter G, Crotty S, Plotkin SA. Correlates of protection against SARS-CoV-2 infection and COVID-19 disease. *Immunol Rev*. 2022;310(1):6–26.
17 Cao Y, Wang J, Jian F, et al. Omicron escapes the majority of existing SARS-CoV-2 neutralizing antibodies. *Nature*. 2022;602(7898):657–663.
18 McMenamin ME, Nealon J, Lin Y, et al. Vaccine effectiveness of one, two, and three doses of BNT162b2 and CoronaVac against COVID-19 in Hong Kong: a population-based observational study. *Lancet Infect Dis*. 2022;22:1435–1443.
19 Le Bert N, Clapham HE, Tan AT, et al. Highly functional virus-specific cellular immune response in asymptomatic SARS-CoV-2 infection. *J Exp Med*. 2021;218(5):e20202617.
20 Jing L, Wu X, Krist MP, et al. T cell response to intact SARS-CoV-2 includes coronavirus cross-reactive and variant-specific components. *JCI Insight*. 2022;7(6):e158126.
21 Moss P. The T cell immune response against SARS-CoV-2. *Nat Immunol*. 2022;23(2):186–193.
22 Ishii H, Nomura T, Yamamoto H, et al. Neutralizing-antibody-independent SARS-CoV-2 control correlated with intranasal-vaccine-induced CD8(+) T cell responses. *Cell Rep Med*. 2022;3(2):100520.
23 Tan AT, Linster M, Tan CW, et al. Early induction of functional SARS-CoV-2-specific T cells associates with rapid viral clearance and mild disease in COVID-19 patients. *Cell Rep*. 2021;34(6):108728.
24 Sekine T, Perez-Potti A, Rivera-Ballesteros O, et al. Robust T cell immunity in convalescent individuals with asymptomatic or mild COVID-19. *Cell*. 2020;183(1):158–168.e14.
25 Bar-On YM, Goldberg Y, Mandel M, et al. Protection by a fourth dose of BNT162b2 against Omicron in Israel. *N Engl J Med*. 2022;386(18):1712–1720.
26 Holm MR, Poland GA. Critical aspects of packaging, storage, preparation, and administration of mRNA and adenovirus-vectored COVID-19 vaccines for optimal efficacy. *Vaccine*. 2021;39(3):457–459.
27 Wang N, Shang J, Jiang S, Du L. Subunit vaccines against emerging pathogenic human coronaviruses. *Front Microbiol*. 2020;11:298.
28 Koff RS. Immunogenicity of hepatitis B vaccines: implications of immune memory. *Vaccine*. 2002;20(31–32):3695–3701.
29 Chen J, Wang J, Zhang J, Ly H. Advances in development and application of influenza vaccines. *Front Immunol*. 2021;12:711997.
30 Fan J, Jin S, Gilmartin L, Toth I, Hussein WM, Stephenson RJ. Advances in infectious disease vaccine adjuvants. *Vaccines*. 2022;10(7):1120.
31 Garcon N, Morel S, Didierlaurent A, Descamps D, Wettendorff M, Van Mechelen M. Development of an AS04-adjuvanted HPV vaccine with the adjuvant system approach. *BioDrugs*. 2011;25(4):217–226.
32 Shi S, Zhu H, Xia X, Liang Z, Ma X, Sun B. Vaccine adjuvants: understanding the structure and mechanism of adjuvanticity. *Vaccine*. 2019;37(24):3167–3178.
33 Lavelle EC, Ward RW. Mucosal vaccines - fortifying the frontiers. *Nat Rev Immunol*. 2022;22(4):236–250.
34 McLachlan JB, Shelburne CP, Hart JP, et al. Mast cell activators: a new class of highly effective vaccine adjuvants. *Nat Med*. 2008;14(5):536–541.
35 St John AL, Choi HW, Walker QD, et al. Novel mucosal adjuvant, mastoparan-7, improves cocaine vaccine efficacy. *NPJ Vaccines*. 2020;5(1):12.
36 McNeil BD, Pundir P, Meeker S, et al. Identification of a mast-cell-specific receptor crucial for pseudo-allergic drug reactions. *Nature*. 2015;519(7542):237–241.
37 Johnson-Weaver BT, Choi HW, Yang H, et al. Nasal immunization with small molecule mast cell activators enhance immunity to co-administered subunit immunogens. *Front Immunol*. 2021;12:730346.
38 Staats HF, Fielhauer JR, Thompson AL, et al. Mucosal targeting of a BoNT/A subunit vaccine adjuvanted with a mast cell activator enhances induction of BoNT/A neutralizing antibodies in rabbits. *PLoS One*. 2011;6(1):e16532.
39 Hassan AO, Kafai NM, Dmitriev IP, et al. A single-dose intranasal ChAd vaccine protects upper and lower respiratory tracts against SARS-CoV-2. *Cell*. 2020;183(1):169–184.e13.
40 Wu S, Zhong G, Zhang J, et al. A single dose of an adenovirus-vectored vaccine provides protection against SARS-CoV-2 challenge. *Nat Commun*. 2020;11(1):4081.
41 Alu A, Chen L, Lei H, Wei Y, Tian X, Wei X. Intranasal COVID-19 vaccines: from bench to bed. *EBioMedicine*. 2022;76:103841.
42 Afkhami S, D'Agostino MR, Zhang A, et al. Respiratory mucosal delivery of next-generation COVID-19 vaccine provides robust protection against both ancestral and variant strains of SARS-CoV-2. *Cell*. 2022;185(5):896–915.e19.
43 Kingstad-Bakke B, Lee W, Chandrasekar SS, et al. Vaccine-induced systemic and mucosal T cell immunity to SARS-CoV-2 viral variants. *Proc Natl Acad Sci U S A*. 2022;119(20):e2118312119.
44 Mao T, Israelow B, Suberi A, et al. Unadjuvanted intranasal spike vaccine booster elicits robust protective mucosal immunity against sarbecoviruses. *bioRxiv*. 2022. https://doi.org/10.1101/2022.01.24.477597.
45 Rathore APS, St John AL. Promises and challenges of mucosal COVID-19 vaccines. *Vaccine*. 2023;41(27):4042–4049.
46 Babicki S, Arndt D, Marcu A, et al. Heatmapper: web-enabled heat mapping for all. *Nucleic Acids Res*. 2016;44(W1):W147–W153.
47 Tan CW, Chia WN, Qin X, et al. A SARS-CoV-2 surrogate virus neutralization test based on antibody-mediated blockage of ACE2-spike protein-protein interaction. *Nat Biotechnol*. 2020;38(9):1073–1078.
48 Tan CW, Chia WN, Young BE, et al. Pan-sarbecovirus neutralizing antibodies in BNT162b2-immunized SARS-CoV-1 survivors. *N Engl J Med*. 2021;385(15):1401–1406.
49 Stadlbauer D, Amanat F, Chromikova V, et al. SARS-CoV-2 seroconversion in humans: a detailed protocol for a serological assay, antigen production, and test setup. *Curr Protoc Microbiol*. 2020;57(1):e100.
50 Mateus J, Grifoni A, Tarke A, et al. Selective and cross-reactive SARS-CoV-2 T cell epitopes in unexposed humans. *Science*. 2020;370(6512):89–94.

51 Brandtzaeg P. Potential of nasopharynx-associated lymphoid tissue for vaccine responses in the airways. *Am J Respir Crit Care Med*. 2011;183(12):1595–1604.
52 Zehn D, Lee SY, Bevan MJ. Complete but curtailed T-cell response to very low-affinity antigen. *Nature*. 2009;458(7235):211–214.
53 Rabenstein H, Behrendt AC, Ellwart JW, et al. Differential kinetics of antigen dependency of CD4+ and CD8+ T cells. *J Immunol*. 2014;192(8):3507–3517.
54 Dong C. Cytokine regulation and function in T cells. *Annu Rev Immunol*. 2021;39:51–76.
55 Wang X, Chan CC, Yang M, et al. A critical role of IL-17 in modulating the B-cell response during H5N1 influenza virus infection. *Cell Mol Immunol*. 2011;8(6):462–468.
56 Imai M, Iwatsuki-Horimoto K, Hatta M, et al. Syrian hamsters as a small animal model for SARS-CoV-2 infection and countermeasure development. *Proc Natl Acad Sci U S A*. 2020;117(28):16587–16595.
57 Sia SF, Yan LM, Chin AWH, et al. Pathogenesis and transmission of SARS-CoV-2 in golden hamsters. *Nature*. 2020;583(7818):834–838.
58 Biji A, Khatun O, Swaraj S, et al. Identification of COVID-19 prognostic markers and therapeutic targets through meta-analysis and validation of Omics data from nasopharyngeal samples. *EBioMedicine*. 2021;70:103525.
59 Merkuleva IA, Shcherbakov DN, Borgoyakova MB, et al. Are hamsters a suitable model for evaluating the immunogenicity of RBD-based anti-COVID-19 subunit vaccines? *Viruses*. 2022;14(5):1060.
60 Sallusto F, Lenig D, Forster R, Lipp M, Lanzavecchia A. Two subsets of memory T lymphocytes with distinct homing potentials and effector functions. *Nature*. 1999;401(6754):708–712.
61 Sigal A, Milo R, Jassat W. Estimating disease severity of Omicron and Delta SARS-CoV-2 infections. *Nat Rev Immunol*. 2022;22(5):267–269.
62 Abdullah F, Myers J, Basu D, et al. Decreased severity of disease during the first global omicron variant covid-19 outbreak in a large hospital in tshwane, south africa. *Int J Infect Dis*. 2022;116:38–42.
63 Mouro V, Fischer A. Dealing with a mucosal viral pandemic: lessons from COVID-19 vaccines. *Mucosal Immunol*. 2022;15(4):584–594.
64 Tioni MF, Jordan R, Pena AS, et al. Mucosal administration of a live attenuated recombinant COVID-19 vaccine protects nonhuman primates from SARS-CoV-2. *NPJ Vaccines*. 2022;7(1):85.
65 Alturaiki W. Considerations for novel COVID-19 mucosal vaccine development. *Vaccines*. 2022;10(8):1173.
66 Americo JL, Cotter CA, Earl PL, Liu R, Moss B. Intranasal inoculation of an MVA-based vaccine induces IgA and protects the respiratory tract of hACE2 mice from SARS-CoV-2 infection. *Proc Natl Acad Sci U S A*. 2022;119(24):e2202069119.
67 Zhu F, Zhuang C, Chu K, et al. Safety and immunogenicity of a live-attenuated influenza virus vector-based intranasal SARS-CoV-2 vaccine in adults: randomised, double-blind, placebo-controlled, phase 1 and 2 trials. *Lancet Respir Med*. 2022;10(8):749–760.
68 Langel SN, Johnson S, Martinez CI, et al. Adenovirus type 5 SARS-CoV-2 vaccines delivered orally or intranasally reduced disease severity and transmission in a hamster model. *Sci Transl Med*. 2022;14:eabn6868.
69 Hoek KL, Greer MJ, McClanahan KG, et al. Granzyme B prevents aberrant IL-17 production and intestinal pathogenicity in CD4(+) T cells. *Mucosal Immunol*. 2021;14(5):1088–1099.
70 Jaffar Z, Ferrini ME, Herritt LA, Roberts K. Cutting edge: lung mucosal Th17-mediated responses induce polymeric Ig receptor expression by the airway epithelium and elevate secretory IgA levels. *J Immunol*. 2009;182(8):4507–4511.
71 de Bree GJ, van Leeuwen EM, Out TA, Jansen HM, Jonkers RE, van Lier RA. Selective accumulation of differentiated CD8+ T cells specific for respiratory viruses in the human lung. *J Exp Med*. 2005;202(10):1433–1442.
72 Ssemaganda A, Nguyen HM, Nuhu F, et al. Expansion of cytotoxic tissue-resident CD8(+) T cells and CCR6(+)CD161(+) CD4(+) T cells in the nasal mucosa following mRNA COVID-19 vaccination. *Nat Commun*. 2022;13(1):3357.
73 Lim JME, Tan AT, Le Bert N, Hang SK, Low JGH, Bertoletti A. SARS-CoV-2 breakthrough infection in vaccinees induces virus-specific nasal-resident CD8+ and CD4+ T cells of broad specificity. *J Exp Med*. 2022;219(10):e20220780.
74 Tang J, Zeng C, Cox TM, et al. Respiratory mucosal immunity against SARS-CoV-2 following mRNA vaccination. *Sci Immunol*. 2022;7:eadd4853.
75 Sallusto F, Langenkamp A, Geginat J, Lanzavecchia A. Functional subsets of memory T cells identified by CCR7 expression. *Curr Top Microbiol Immunol*. 2000;251:167–171.
76 Abdelsamed HA, Moustaki A, Fan Y, et al. Human memory CD8 T cell effector potential is epigenetically preserved during in vivo homeostasis. *J Exp Med*. 2017;214(6):1593–1606.
77 Moskowitz DM, Zhang DW, Hu B, et al. Epigenomics of human CD8 T cell differentiation and aging. *Sci Immunol*. 2017;2(8):eaag0192.
78 Kumar BV, Connors TJ, Farber DL. Human T cell development, localization, and function throughout life. *Immunity*. 2018;48(2):202–213.
79 Ahmed R, Bevan MJ, Reiner SL, Fearon DT. The precursors of memory: models and controversies. *Nat Rev Immunol*. 2009;9(9):662–668.
80 Cyster JG, Allen CDC. B cell responses: cell interaction dynamics and decisions. *Cell*. 2019;177(3):524–540.
81 Song W, Craft J. T follicular helper cell heterogeneity: TIME, space, and function. *Immunol Rev*. 2019;288(1):85–96.
82 Morita R, Schmitt N, Bentebibel SE, et al. Human blood CXCR5(+) CD4(+) T cells are counterparts of T follicular cells and contain specific subsets that differentially support antibody secretion. *Immunity*. 2011;34(1):108–121.
83 MacLeod MK, David A, McKee AS, Crawford F, Kappler JW, Marrack P. Memory CD4 T cells that express CXCR5 provide accelerated help to B cells. *J Immunol*. 2011;186(5):2889–2896.
84 Locci M, Havenar-Daughton C, Landais E, et al. Human circulating PD-1+CXCR3-CXCR5+ memory Tfh cells are highly functional and correlate with broadly neutralizing HIV antibody responses. *Immunity*. 2013;39(4):758–769.
85 Robinson AM, Higgins BW, Shuparski AG, Miller KB, McHeyzer-Williams LJ, McHeyzer-Williams MG. Evolution of antigen-specific follicular helper T cell transcriptional programs across effector function and through to memory. *bioRxiv*. 2021, 2021.09.17.460841.
86 Lentschat A, Karahashi H, Michelsen KS, et al. Mastoparan, a G protein agonist peptide, differentially modulates TLR4- and TLR2-mediated signaling in human endothelial cells and murine macrophages. *J Immunol*. 2005;174(7):4252–4261.
87 St John AL, Rathore APS, Ginhoux F. New perspectives on the origins and heterogeneity of mast cells. *Nat Rev Immunol*. 2022;23:55–68.
88 Keech C, Albert G, Cho I, et al. Phase 1-2 trial of a SARS-CoV-2 recombinant spike protein nanoparticle vaccine. *N Engl J Med*. 2020;383(24):2320–2332.
89 Hernandez-Bernal F, Ricardo-Cobas MC, Martin-Bauta Y, et al. A phase 3, randomised, double-blind, placebo-controlled clinical trial evaluation of the efficacy and safety of a SARS-CoV-2 recombinant spike RBD protein vaccine in adults (ABDALA-3 study). *Lancet Reg Health Am*. 2023;21:100497.
90 Acharya CB, Schrom J, Mitchell AM, et al. Viral load among vaccinated and unvaccinated, asymptomatic and symptomatic persons infected with the SARS-CoV-2 delta variant. *Open Forum Infect Dis*. 2022;9(5):ofac135.
91 Mastrorosa I, Cozzi-Lepri A, Colavita F, et al. SARS-CoV-2 nasopharyngeal viral load in individuals infected with BA.2, compared to Alpha, Gamma, Delta and BA.1 variants: a single-center comparative analysis. *J Clin Virol*. 2022;157:105299.
92 McEllistrem MC, Clancy CJ, Buehrle DJ, Lucas A, Decker BK. Single dose of an mRNA severe acute respiratory syndrome coronavirus 2 (SARS-Cov-2) vaccine is associated with lower nasopharyngeal viral load among nursing home residents with asymptomatic coronavirus disease 2019 (COVID-19). *Clin Infect Dis*. 2021;73(6):e1365–e1367.
93 Li H, Li Y, Liu J, Liu J, Han J, Yang L. Vaccination reduces viral load and accelerates viral clearance in SARS-CoV-2 Delta variant-infected patients. *Ann Med*. 2023;55(1):419–427.
94 Network H-R, Thompson MG, Yoon SK, et al. Association of mRNA vaccination with clinical and virologic features of COVID-19 among US Essential and Frontline workers. *JAMA*. 2022;328(15):1523–1533.